

1 **Short title:** MdSIZ1 promotes Fe homeostasis

2

3

4 **Corresponding author:** Yu-Jin Hao

5

6

7 **Article Title:** The SUMO E3 ligase MdSIZ1 targets MdbHLH104 to regulate plasma
8 membrane H⁺-ATPase activity and iron homeostasis

9

10

11 **Author:** Li-Jie Zhou¹, Chun-Ling Zhang¹, Rui-Fen Zhang^{1,2}, Gui-Luan Wang¹,
12 Yuan-Yuan Li¹, Yu-Jin Hao^{1*}

13 ¹ State Key Laboratory of Crop Biology, National Research Center for Apple
14 Engineering and Technology, College of Horticulture Science and Engineering,
15 Shandong Agricultural University, Tai-An, Shandong 271018, China.

16 ² Qingdao Academy of Agricultural Science, Qing-Dao, Shandong 266100, China.

17

18 **One sentence summary:** The SUMO E3 ligase MdSIZ1 sumoylates and stabilizes
19 MdbHLH104 to increase PM H⁺-ATPase mediated rhizosphere acidification and Fe
20 acquisition under conditions of Fe deficiency in apple.

21

22

23 **Author Contributions:** Y.J.H. and L.J.Z. conceived and designed the experiments;
24 L.J.Z. performed most of the experiments; C.L.Z., R.F.Z., G.L.W. and Y.Y.L provided
25 technical assistance; L.J.Z. and Y.J.H. analyzed the data and wrote the manuscript.

26

27

28 **Funding information:** This work was financially supported by grants from the
29 National Natural Science Foundation of China (31430074 and 31772275), the
30 Ministry of Education of China (IRT15R42), the Ministry of Agriculture of China
31 (CARS-28) and Shandong Province (SDAIT-06-03).

32

33 **Corresponding author email:** haoyujin@sdau.edu.cn

34 **Abstract**

35 SIZ1-mediated SUMO modification of target proteins is important for various
36 biological processes related to abiotic stress resistance in plants; however, little is
37 known about its role in resistance toward iron (Fe) deficiency. Here, the SUMO E3
38 ligase MdsIZ1 was shown to be involved in the plasma membrane (PM)
39 H⁺-ATPase-mediated response to Fe deficiency. Subsequently, a basic
40 helix-loop-helix (bHLH) transcription factor (TF), MdbHLH104, which acts as a key
41 component in regulating PM H⁺-ATPase-mediated rhizosphere acidification and Fe
42 uptake in apples (*Malus domestica*), was identified as a direct target of MdsIZ1.
43 MdsIZ1 directly sumoylated MdbHLH104 both *in vitro* and *in vivo*, especially under
44 conditions of Fe deficiency, and this sumoylation was required for MdbHLH104
45 protein stability. Double substitution of K139R and K153R in MdbHLH104 blocked
46 MdsIZ1-mediated sumoylation *in vitro* and *in vivo*, indicating that the K139 and
47 K153 residues were the principal sites of SUMO conjugation. Moreover, the transcript
48 level of the *MdsIZ1* gene was substantially induced following Fe deficiency. *MdsIZ1*
49 overexpression exerted a positive influence on PM H⁺-ATPase-mediated rhizosphere
50 acidification and Fe uptake. Our findings reveal an important role for sumoylation in
51 the regulation of PM H⁺-ATPase-mediated rhizosphere acidification and Fe uptake
52 during Fe deficiency in plants.

53

54 **Keywords:** Plasma membrane H⁺-ATPase; Fe homeostasis; SUMO E3 ligase; bHLH
55 transcription factors; post-translational modification.

56

57 **Introduction**

58 Iron (Fe) is one of the most important micronutrients in both plants and humans.
59 In plants, Fe acts as a cofactor for a wide variety of proteins participating in many
60 cellular functions, such as hormone biosynthesis, photosynthesis, nitrogen fixation,
61 and mitochondrial respiration (Hänsch and Mendel, 2009). Moreover, Fe deficiency is
62 one of the major causes of anemia in humans, and a diet rich in plants can be a major
63 source of Fe. Importantly, even when the Fe content in the topsoil is high, Fe

64 deficiency in plants is still common, as it generally exists as insoluble ferric
65 hydroxides in the soil. As such, low-Fe stress can be a major factor limiting crop yield
66 and quality.

67 To cope with conditions of Fe deficiency, angiosperms have evolved two distinct
68 strategies. In dicotyledonous plants and non-graminaceous monocot species, the
69 extrusion of protons mediated by plasma membrane (PM) H⁺-ATPases acidifies the
70 soil to make Fe(III) more soluble. Subsequently, FRO2 (FERRIC REDUCTASE
71 OXIDASE 2) converts Fe³⁺ to Fe²⁺, which is then transported into the roots via IRT1
72 (IRON REGULATED TRANSPORTER 1) (Hell and Stephan, 2003; Curie and Briat,
73 2003; Hindt and Guerinot, 2012; Walker and Connolly, 2008). In contrast,
74 graminaceous plants release phytosiderophores to chelate Fe from the soil. The
75 resultant chelated complexes are then imported into root epidermal cells via a specific
76 transport system (Mori, 1999; Kobayashi et al., 2010).

77 Transcriptional regulation is one of the most common ways to regulate the
78 function of genes involved in Fe homeostasis under Fe-deficient conditions. A number
79 of transcription factors (TFs), such as the basic helix-loop-helix (bHLH) TFs, have
80 been identified to positively regulate Fe deficiency response (Kobayashi and
81 Nishizawa, 2012). The first subgroup Ib bHLH protein characterized from plants was
82 FER in tomato (*Solanum lycopersicum*) (Ling et al., 2002). Its Arabidopsis
83 (*Arabidopsis thaliana*) ortholog FIT (FER-LIKE IRON DEFICIENCY-INDUCED
84 TRANSCRIPTION FACTOR) controls ferric reduction response and Fe transport into
85 the plant root by directly regulating the transcription of the *FRO2* and *IRT1* genes
86 under the conditions of Fe deficiency (Colangelo and Guerinot, 2004; Yuan et al.,
87 2005, 2008). What's more, FIT can form a heterodimer with other members of the Ib
88 subgroup of bHLH TFs, including bHLH38/39/100/101, to constitutively activate
89 *IRT1* and *FRO2* (Yuan et al., 2008; Wang et al., 2013). In addition to those of the Ib
90 subgroup, IVc subgroup bHLH TFs also influence Fe homeostasis under Fe-deficient
91 conditions. For example, the PYE bHLH protein was up-regulated by Fe-deficient
92 conditions. The Fe transport-related genes *NAS4* (*NICOTIANAMINE SYNTHASE4*),
93 *ZIF1* (*ZINC-INDUCED FACILITATOR1*), and *FRO3* were up-regulated in the *pye-1*

94 mutant under Fe-deficient conditions, suggesting PYE functions as a negative
95 regulator of the Fe deficiency response (Long et al., 2010). Most recently, Zhang et al.
96 (2015) reported that the IVc subgroup bHLH TFs bHLH104 and bHLH105 formed a
97 heterodimer to positively regulate Fe deficiency response by directly activating the
98 transcription of genes encoding the Ib bHLH TFs bHLH38/39/100/101. What's more,
99 AtbHLH104 also regulates the acidification of rhizospheres under Fe-deficient
100 conditions (Zhang et al., 2015).

101 Plant PM H⁺-ATPases are composed of a series of proton pumps that are driven
102 by ATP hydrolysis, providing an energy source to transport nutrients into plant cells
103 by generating electrochemical gradients (Haruta and Sussman, 2012). In Fe deficiency
104 responses, PM H⁺-ATPases play a crucial role in the first step towards improving the
105 plant's ability to acquire Fe from the soil in response to low Fe, especially in
106 dicotyledonous plants. In Arabidopsis, there are a total of 11 *AHA* genes that encode
107 functional PM H⁺-ATPase proteins that respond to various environmental stimuli
108 (Palmgren, 2001). Among them, *AHA2*, *AHA3*, *AHA4*, and *AHA7* are transcriptionally
109 inducible by low-Fe stress, and *AHA2* is involved in rhizosphere acidification (Santi
110 and Schmidt, 2009). Among the 18 apple (*Malus domestica*) MdAHAs, MdAHA1,
111 MdAHA3, MdAHA7, MdAHA8, MdAHA9, MdAHA11, and MdAHA12 are closely
112 related to AtAHA2, and MdAHA8 plays an important role in Fe homeostasis (Zhao et
113 al., 2016 a).

114 In plants, PM H⁺-ATPases are regulated by various factors at different levels. At
115 the post-translational level, PM H⁺-ATPases can be activated by phosphorylation. For
116 example, PM H⁺-ATPase *AHA2* in Arabidopsis, which is mainly responsible for
117 rhizosphere acidification under iron deficiency, is phosphorylated at Ser-931 in the
118 C-terminal regulatory domain by protein kinase PKS5. The phosphorylation of this
119 site inhibits the interaction between *AHA2* and an activating 14-3-3 protein, resulting
120 in inhibited PM H⁺-ATPase activity (Fuglsang et al., 2007). In addition, SAUR
121 proteins, which are positive effectors of cell expansion, are rapidly induced by auxin
122 and serve to negatively regulate PP2C-D phosphatases. Subsequently, the decreased
123 PP2C-D activity alters phosphorylation of PM H⁺-ATPases, which promotes cell

124 expansion through an acid growth mechanism (Spartz et al., 2014). Moreover,
125 aluminum stress promotes phosphorylation of PM H⁺-ATPases and their binding with
126 14-3-3 proteins in black soybeans (*Glycinemax (L.) merr*) (Guo et al., 2013).

127 In addition to post-translational modification, transcriptional regulation is a
128 common manner by which cells modulate the activity of PM H⁺-ATPases. Many
129 transcription factors are found to regulate PM H⁺-ATPase in plants. For example, the
130 expression and activity of AtAHA2 are positively regulated by GsERF71, a TF of the
131 AP2/ERF family from wild soybean (*Glycine soja*), in response to alkaline stress (Yu
132 et al., 2017). Additionally, bHLH TFs associated with Fe homeostasis are also
133 involved in the regulation of PM H⁺-ATPase gene transcription. For example, the
134 *Chrysanthemum (Chrysanthemum morifolium)* bHLH TF CmbHLH1 enhances the
135 activity of H⁺-ATPase CmHA to promote rhizosphere acidification and Fe
136 homeostasis (Zhao et al., 2014). Recently, it was found that the IVc subgroup bHLH
137 TF MdbHLH104, the apple homolog of AtbHLH104, directly binds to the promoter of
138 the *MdAHA8* gene to activate PM H⁺-ATPase activity in response to Fe deficiency
139 (Zhao et al., 2016 a).

140 Furthermore, regulators that act up-stream of these TFs to modulate PM
141 H⁺-ATPase activity and Fe homeostasis have also been identified. MdbT1 and
142 MdbT2 belong to the BTB/TAZ family of proteins. They recruit the MdbTs^{MdCUL3} E3
143 ligase complex to target MdbHLH104 for ubiquitination to promote its degradation
144 via a 26S proteasome pathway (Zhao et al., 2016 b). Similarly, an E3 ubiquitin ligase
145 BTS interacts with bHLH104 and ILR3 (also called bHLH105) and negatively
146 regulates Fe absorption (Selote et al., 2015; Zhang et al., 2015). Degradation of TFs
147 that positively regulate PM H⁺-ATPase activity and Fe uptake protects plants from
148 injury caused by generation of Fe overload-associated reactive oxygen species (ROS)
149 (Zhao et al., 2016 b).

150 The conjugation of small ubiquitin-like modifier (SUMO) to target proteins is
151 another important post-translational modification that, in most cases, serves to
152 antagonize the effects of ubiquitination of target proteins (Ulrich, 2005). In plants,

153 sumoylation is an important post-translational modification of substrate proteins that
154 involves three enzymatic steps catalyzed by a single E1 SUMO-activating enzyme
155 (SAE1 and SAE2 as its subunits), a single E2-conjugating enzyme, SCE1, and two
156 classes of E3 ligase enzymes, including MMS21 and SIZ1 (Miura et al. 2005; Huang
157 et al. 2009; Ishida et al. 2012; Novatchkova et al. 2012). SUMO modification of
158 substrate proteins mediated by SIZ1 mediates various biological processes related to
159 nutrient acquisition and abiotic stresses. For example, in Arabidopsis, SIZ1 positively
160 controls nitrogen assimilation by directly sumoylating the nitrate reductases NIA1 and
161 NIA2 (Park et al., 2011); Heterologous expression of *OsSIZ1*, a rice (*Oryza sativa*)
162 SUMO E3 ligase, enhances broad abiotic stress tolerance and mineral uptake in
163 transgenic creeping bentgrass (*Agrostis stolonifera* L.) (Li et al., 2013). In Arabidopsis,
164 SIZ1 targets PHR1 and ABI5 proteins for SUMO modification to regulate the
165 phosphate deficiency response and ABA signaling (Miura et al., 2005; Miura et al.,
166 2009). Interestingly, PM H⁺-ATPases are involved in many abiotic stress responses
167 that are associated with SIZ1-mediated sumoylation, such as the phosphate starvation
168 response and ABA response (Andersen et al., 2007; Yuan et al., 2017). However, it is
169 largely unknown if and/or how SIZ1-mediated sumoylation regulates PM H⁺-ATPases
170 in response to abiotic stresses, such as Fe deficiency.

171 In this study, MdbHLH104, an up-stream regulator of the PM H⁺-ATPase gene
172 *MdAHA8* was identified via yeast two-hybrid as an MdSIZ1-interacting protein.
173 MdSIZ1 was further characterized as having functions in sumoylation and affecting
174 the stability of the MdbHLH104 protein. Finally, the molecular mechanism by which
175 MdSIZ1 regulates PM H⁺-ATPase-mediated rhizosphere acidification during Fe
176 homeostasis is summarized and discussed.

177

178

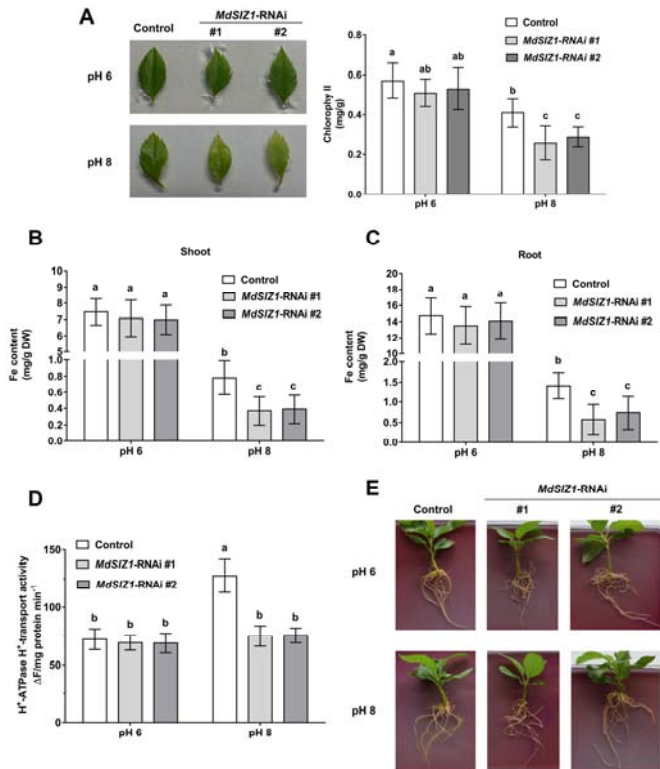
179 **Results**

180 **The SUMO E3 ligase MdSIZ1 is involved in the PM H⁺-ATPase-mediated**
181 **response to Fe deficiency**

182 To examine if MdSIZ1 is involved in response to Fe deficiency, RT-qPCR was
183 conducted. Our analysis showed that transcript levels of *MdSIZ1* were elevated by Fe
184 deficiency treatment (Supplemental Fig S1A). To confirm the result,
185 anti-MdSIZ1-specific antibodies were custom made (Supplemental Fig S1B) and used
186 for detection of MdSIZ1 protein levels by western blot assays. The result showed that
187 the protein abundance of MdSIZ1 increased with Fe deficiency in 'Gala' apple plants
188 (Supplemental Fig S1C and S1D). Together, these observations suggest that MdSIZ1
189 functions as an important protein in response to Fe deficiency in apples.

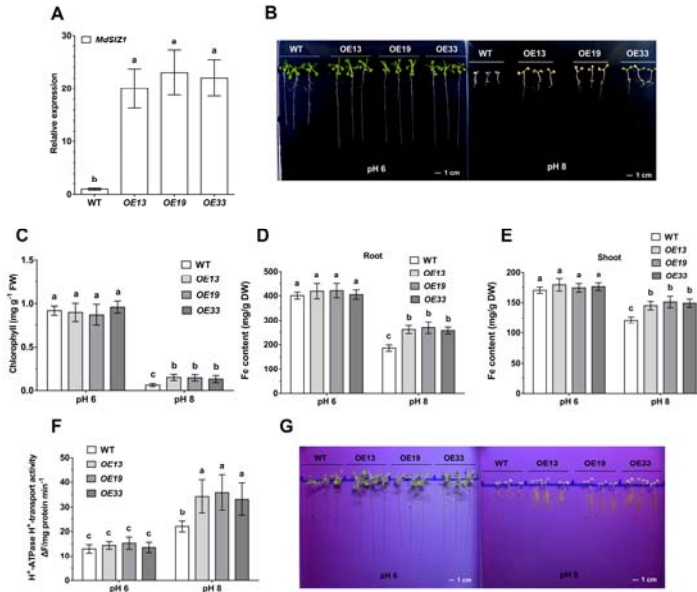
190 In soil, for each unit increase in pH, Fe solubility decreases up to 1000-fold (Santi
191 and Schmidt, 2009). To examine whether MdSIZ1 regulates PM H⁺-ATPase-mediated
192 rhizosphere acidification and Fe homeostasis in apples, an *MdSIZ1* RNAi vector
193 containing a 35S:DsRED1 cassette was constructed and transiently transformed into
194 the root cells of 'Gala' apple via *Agrobacterium rhizogenes*-mediated genetic
195 transformation, while an empty vector was used as a control. The *MdSIZ1* transcripts
196 were remarkably downregulated in the roots of these plants (Supplemental Fig S2),
197 indicating that chimeric plants composed of transgenic roots and wild-type (WT)
198 shoots were successfully obtained. Two batches of chimeric transgenic plants denoted
199 as #1 and #2 were used to detect Fe acquisition and PM H⁺-ATPase H⁺-transport
200 activity. The results showed that chimeric plants with transgenic *MdSIZ1*-RNAi roots
201 exhibited more serious leaf chlorosis in pH 8.0 alkaline medium than those with the
202 control roots, while none of the plants showed leaf chlorosis in pH 6.0 normal
203 medium (Fig. 1A).

204 Furthermore, Fe contents were measured in the shoots and roots, respectively. It
205 was found that chimeric transgenic plants grown in pH 8.0 medium, but not in pH 6.0
206 medium, accumulated 52% less Fe in their shoots and 59% less in their roots
207 compared with empty vector controls (Fig. 1B and 1C). Subsequently, PM H⁺-ATPase
208 H⁺-transport activity was assessed. The results showed that transgenic *MdSIZ1*-RNAi



209 roots grown in pH 8.0 medium exhibited lower PM H⁺-ATPase H⁺-transport activity
 210 than the empty vector controls (Fig. 1D). Finally, it was found that transgenic
 211 *MdsIZ1*-RNAi roots grown in pH 8.0 medium released less H⁺ than the empty vector
 212 controls, as indicated by the yellow color around the roots after staining with
 213 bromocresol purple (Fig. 1E).

214 As it is difficult to obtain transgenic apple plants overexpressing *MdsIZ1*, *MdsIZ1*
 215 was ectopically expressed in *Arabidopsis* to further characterize if *MdsIZ1* functions
 216 in the regulation of the PM H⁺-ATPase-mediated response to Fe acquisition *in planta*.
 217 Three independent transgenic lines, OE13, OE19, and OE33, were chosen for further
 218 analysis (Fig. 2A). When allowed to grow in pH 6.0 medium, transgenic seedlings
 219 exhibited longer roots than the WT controls, but no other phenotype was observed.
 220 When grown in pH 8.0 medium, transgenic seedlings exhibited a higher tolerance to
 221 Fe deficiency, as indicated by more growth, than the WT controls. Moreover, in pH
 222 8.0 medium, these transgenic seedlings produced more chlorophyll, accumulated
 223 more Fe, exhibited greater PM H⁺-ATPase H⁺-transport activity, and released more H⁺
 224 into the medium than the WT controls (Fig. 2B-G).

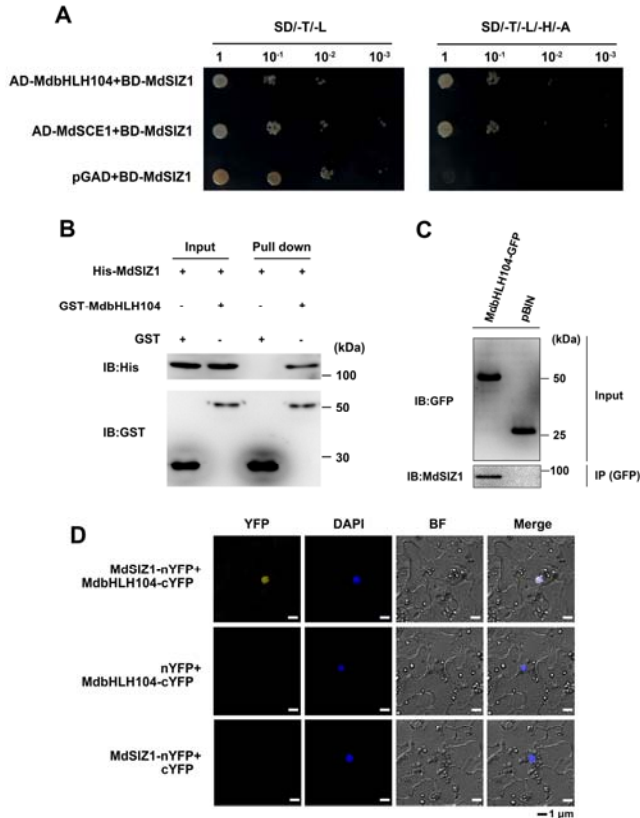


225 In addition, the results from assessment of apple calli showed that the
 226 overexpression of *MdsIZ1* resulted in higher PM H⁺-ATPase H⁺-transport activity
 227 compared with WT and the controls, while *MdsIZ1* suppression lowered this activity,
 228 leading to a similar trend in Fe acquisition under alkaline conditions as observed in
 229 the transgenic Arabidopsis plants (Supplemental Fig S3). Taken together, these results
 230 indicated that *MdsIZ1* plays an important role in the regulation of PM
 231 H⁺-ATPase-mediated acidification capacity and Fe acquisition in plants.

232 ***MdsIZ1* interacts with *MdbHLH104* both *in vitro* and *in vivo***

233 To investigate how *MdsIZ1* regulates PM H⁺-ATPase-mediated acidification capacity
 234 and Fe acquisition, a yeast two-hybrid (Y2H) screen was performed to identify
 235 *MdsIZ1*-interacting proteins. As a result, several positive colonies were obtained. One
 236 of them contained a partial cDNA fragment of the *MdbHLH104* gene, which was
 237 previously reported to be a positive regulator of PM H⁺-ATPase activity in apple
 238 plants (Supplemental Fig S4A; Zhao et al., 2016 a).

239 Y2H assays were conducted to confirm that *MdsIZ1* interacts with the full length
 240 *MdbHLH104* protein. *MdsCE1* (SUMO E2 Conjugating Enzyme 1), which is a
 241 homolog of *AtSCE1*, and a pGAD empty vector were used as positive and negative
 242 controls, respectively. Yeast cells co-expressing AD-*MdbHLH104*+BD-*MdsIZ1* or
 243 AD-*MdsCE1*+BD-*MdsIZ1*, but not those co-expressing pGAD+BD-*MdsIZ1*, grew



244 on SD/-Trp/-Leu/-His/-Ade screening medium (Fig. 3A), indicating that MdsIZ1
 245 interacted with MdbHLH104 in yeast cells.

246 Importantly, MdsIZ1 did not interact with other IVc subgroup bHLH transcription
 247 factors, such as MdbHLH105, MdbHLH115, MdbHLH11, MdbHLH121, or MdPYE,
 248 which are reported to be involved in the regulation of Fe homeostasis (Supplemental
 249 Fig. S4B; Zhao et al., 2016 a). Therefore, MdsIZ1 specifically interacted with
 250 MdbHLH104 in yeast cells.

251 The physical interaction between MdsIZ1 and MdbHLH104 was further
 252 confirmed using an *in vitro* pull-down assay. The results showed that His-MdsIZ1 and
 253 GST-MdbHLH104 were both detected in whole-cell lysates (Input). MdsIZ1 was not
 254 detected in the control sample (GST protein alone), whereas MdsIZ1 fused with a His
 255 tag was pulled down via GST-MdbHLH104 (Fig. 3B), indicating that MdsIZ1
 256 directly interacted with MdbHLH104.

257 To further confirm their interaction *in vivo*, a co-immunoprecipitation (Co-IP)
 258 assay was performed. Total proteins extracted from *35S:MdbHLH104-GFP*

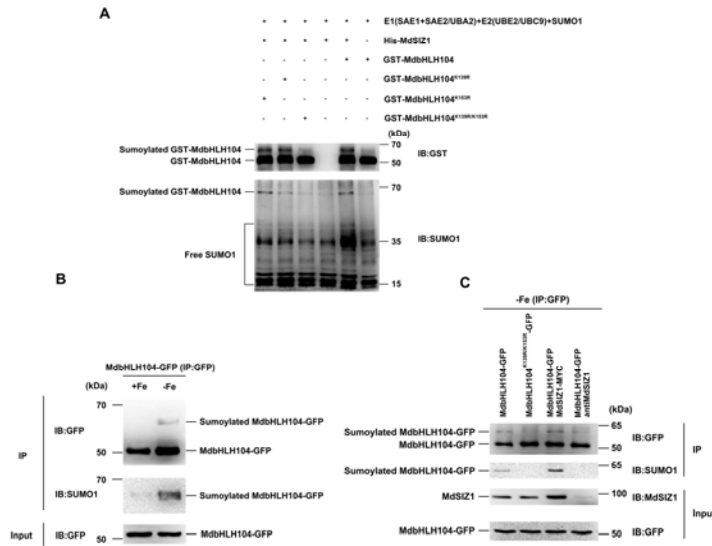
259 (*MdbHLH104-GFP*) and *35S:GFP* (pBIN) transgenic apple plants (Zhao et al., 2016 a)
260 were used to carry out the immunoprecipitation using anti-GFP antibodies. As a result,
261 MdSIZ1 was detected in the pellet fraction (IP) of *MdbHLH104-GFP* transgenic
262 plants but not in that of the pBIN control (Fig. 3C), indicating that MdSIZ1 interacted
263 with MdbHLH104 *in vivo*.

264 Bimolecular fluorescence complementation (BiFC) assays were also employed to
265 examine the MdSIZ1-MdbHLH104 interaction *in planta*. The *MdbHLH104* gene
266 sequence fused in frame with the 5' end of a gene sequence encoding the C-terminal
267 half of yellow fluorescent protein (MdbHLH104-cYFP) and the MdSIZ1 gene
268 sequence fused in frame with the 3' end of a gene sequence encoding the N-terminal
269 half of YFP (MdSIZ1-nYFP) were transiently co-expressed in tobacco leaves. It was
270 found that MdSIZ1 interacted with MdbHLH104 in the nucleus (Figure 3D),
271 indicating that MdSIZ1 and MdbHLH104 colocalize inside the cell.

272 Taken together, these observations indicate that MdSIZ1 interacts with
273 MdbHLH104 both *in vitro* and *in vivo*.

274 **MdSIZ1 directly sumoylates MdbHLH104 proteins at residues K139 and K153** 275 **under conditions of Fe deficiency**

276 Considering MdSIZ1 functions as a SUMO E3 ligase (Zhou et al., 2017) and that it
277 interacts with MdbHLH104, it is reasonable to hypothesize that MdSIZ1 may directly
278 sumoylate the MdbHLH104 protein. Subsequently, the putative sumoylation site
279 consensus sequence ϕ -K-X-E/D (ϕ represents a hydrophobic amino acid, K represents
280 the lysine that is conjugated to SUMO, X represents any amino acid, and E/D
281 represents an acidic residue) (Sampson et al., 2001) was identified in MdbHLH104
282 using SUMOplot (<http://www.abgent.com/sumoplot>) analysis (Lin et al., 2016). It was
283 found that two sumoylation sites with high conservation among different plant species
284 exist in MdbHLH104 (LK139AE and LK153AD), suggesting that it may be a SUMO
285 substrate (Supplemental Fig. S5). To test whether MdbHLH104 is a substrate of
286 MdSIZ1, an *in vitro* sumoylation assay was performed. Recombinant
287 GST-MdbHLH104 was incubated with SUMO-activating enzyme E1,
288 SUMO-conjugating enzyme E2, SUMO1, and recombinant His-MdSIZ1, followed by



289 immunoblot analysis. The results showed that SUMO1-MdbHLH104 conjugates were
 290 not detected by either anti-GST or anti-SUMO1 antibodies in the absence of MdSIZ1,
 291 but conjugates were detected when all components were present (Fig. 4A), indicating
 292 that MdSIZ1 directly sumoylated MdbHLH104 *in vitro*. In addition, the single
 293 substitution of K-to-R of either the K139 or K153 site did not block the
 294 MdbHLH104-SUMO1 conjugation; however, double substitution at both sites did
 295 block conjugation, indicating that both K139 and K153 were crucial sites for SUMO
 296 conjugation of MdbHLH104.

297 To examine whether Fe deficiency could induce sumoylation of MdbHLH104
 298 proteins, *MdbHLH104-GFP* transgenic plants of line L1 were used (Zhao et al., 2016
 299 a). MdbHLH104-GFP proteins extracted from transgenic plants treated with or
 300 without Fe deficiency were immunoprecipitated with an anti-GFP antibody and then
 301 subjected to western blot analysis with anti-GFP and anti-SUMO1 antibodies,
 302 respectively. The result showed that the MdbHLH104 protein exhibited higher
 303 sumoylation levels under Fe-deficient conditions than under Fe-sufficient conditions
 304 (Fig. 4B), indicating that Fe deficiency could induce SUMO modification of
 305 MdbHLH104 proteins in apple plants.

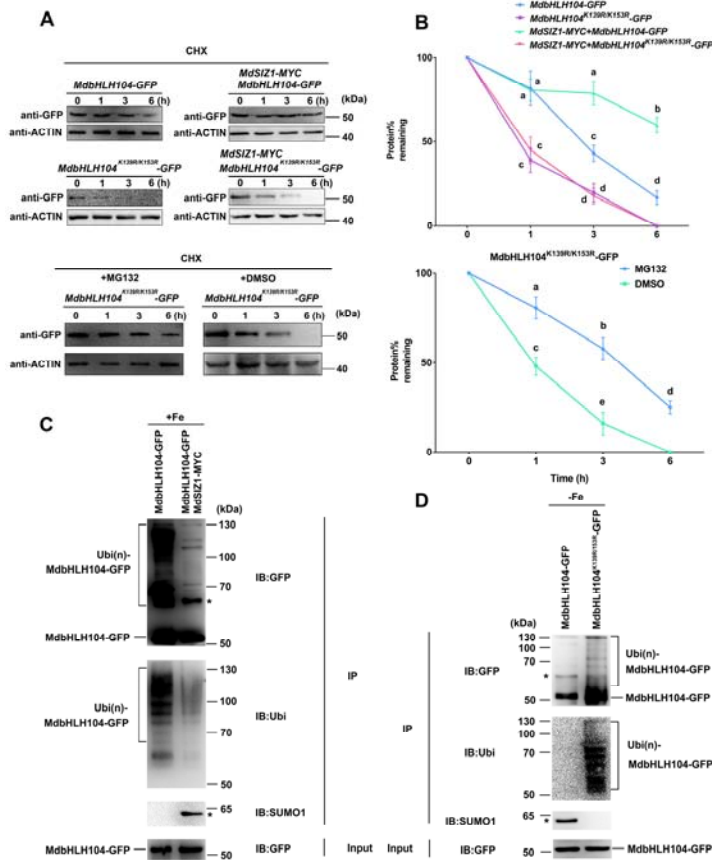
306 To examine whether amino acids K139 and K153 were crucial for Fe-induced
 307 sumoylation of MdbHLH104 *in vivo*, transgenic apple calli *MdbHLH104-GFP* and
 308 *MdbHLH104^{K139R/K153R}-GFP* were obtained and used for sumoylation detection

309 (Supplemental Fig. S6B and S6C). The result showed that Fe deficiency induced
310 SUMO modification of MdbHLH104 proteins in apple calli, similar to that observed
311 in transgenic plants, and that double mutation of K139R/K153R in the MdbHLH104
312 protein abolished this sumoylation (Fig. 4C), indicating that K139 and K153 were
313 crucial for Fe deficiency-induced sumoylation of MdbHLH104. In addition, double
314 transgenic calli *MdbHLH104-GFP/MdSIZ1-MYC* and *MdbHLH104-GFP/antiMdSIZ1*
315 were obtained (Supplemental Fig. S6B and S6C). It was found that *MdSIZ1*
316 overexpression enhanced the sumoylation levels of the MdbHLH104 protein in
317 response to Fe deficiency, while its suppression remarkably decreased the
318 sumoylation levels (Fig. 4C), suggesting that MdSIZ1 was involved in Fe
319 deficiency-induced sumoylation of the MdbHLH104 protein.

320 **MdSIZ1 stabilizes MdbHLH104 and inhibits its ubiquitination**

321 To further investigate how MdSIZ1 influences MdbHLH104, protein degradation
322 assays were performed. After pretreatment in Fe-deficient conditions for 1 h, four
323 types of transgenic calli, *MdbHLH104-GFP*, *MdbHLH104-GFP/MdSIZ1-MYC*,
324 *MdbHLH104^{K139R/K153R}-GFP*, and *MdbHLH104^{K139R/K153R}-GFP/MdSIZ1-MYC*, were
325 treated under Fe-sufficient conditions for different durations. The results showed that
326 the substitution of K-to-R of residues K139 and K153 clearly increased the
327 degradation rate of the MdbHLH104-GFP proteins (Fig. 5A and 5B). In addition,
328 *MdSIZ1* overexpression inhibited the proteolysis of MdbHLH104-GFP, but not
329 MdbHLH104^{K139R/K153R}-GFP, indicating that MdSIZ1-mediated sumoylation of the
330 MdbHLH104-GFP protein promoted its abundance.

331 To exclude the possibility that the observed change in MdbHLH104 protein levels
332 was a result of variation in transcription levels, an RT-qPCR assay was performed
333 using *MdSIZ1*-overexpression and *MdSIZ1*-suppression transgenic calli. The data
334 indicated that there was no difference in the transcript levels of *MdbHLH104* in WT,
335 *MdSIZ1-OE*, or *antiMdSIZ1* transgenic calli in both Fe-sufficient and Fe-deficient
336 conditions (Supplemental Fig. S7), suggesting that MdSIZ1 affected MdbHLH104
337 abundance at the protein level. Taken together, these results indicated that
338 MdSIZ1-mediated sumoylation at residues K139 and K153 of MdbHLH104 promotes



339 its stability.

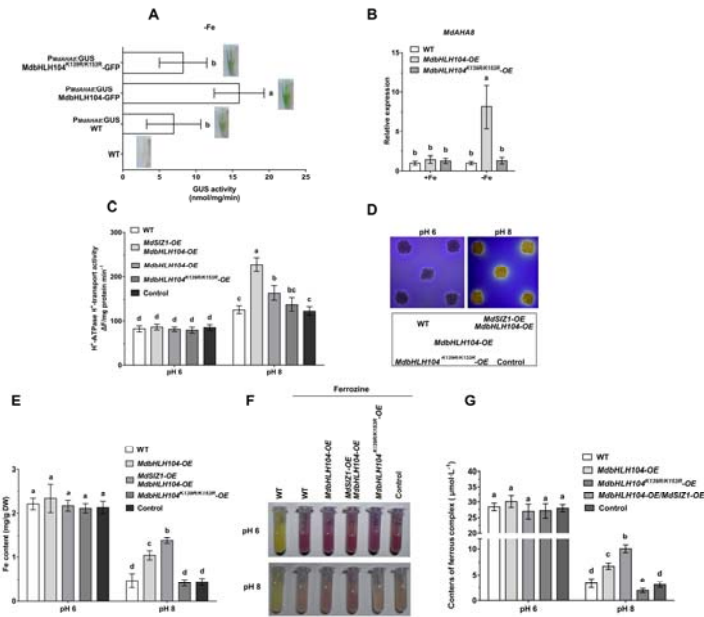
340 In addition, treatment with the 26S proteasome inhibitor MG132 noticeably
 341 inhibited the degradation of the MdbHLH104 proteins caused by the mutation of
 342 sumoylation sites (Fig. 5A and 5B), indicating that MdsIZ1 may stabilize the
 343 MdbHLH104 protein by inhibiting its proteolysis via the 26S proteasome, which is
 344 generally associated with ubiquitin modifications. To determine whether
 345 MdsIZ1-mediated sumoylation influences MdbHLH104 protein ubiquitination,
 346 MdbHLH104 proteins were immunoprecipitated with anti-GFP antibodies from three
 347 types of transgenic calli, *MdbHLH104-GFP*, *MdbHLH104-GFP/MdsIZ1-MYC*, and
 348 *MdbHLH104^{K139R/K153R}-GFP*, followed by western blot analysis. The result indicated
 349 that the *MdbHLH104-GFP* transgenic calli generated more high-molecular-mass
 350 forms of MdbHLH104-GFP under Fe-sufficient conditions than under Fe-deficient
 351 conditions (Fig. 5C and 5D). However, overexpression of *MdsIZ1* in the
 352 *MdbHLH104-GFP* background inhibited this ubiquitination (Fig. 5C). In contrast,

353 mutation of the sumoylation sites in MdbHLH104-GFP clearly promoted its ubiquitin
354 modification under conditions of Fe deficiency (Fig. 5D). Thus, MdSIZ1-mediated
355 sumoylation of MdbHLH104 inhibited its ubiquitination.

356 **MdbHLH104 sumoylation at residues K139 and K153 is crucial for its function**
357 **in activating *MdAHA8* transcription and promoting Fe acquisition.**

358 To examine whether the sumoylation of MdbHLH104 was required for its function in
359 activating the transcription of *MdAHA8*, a *pMdAHA8:GUS* construct was genetically
360 transformed into apple calli. Subsequently, the constructs *MdbHLH104-GFP* and
361 *MdbHLH104^{K139R/K153R}-GFP* were introduced into *pMdAHA8:GUS* transgenic calli
362 (Supplemental Fig. S6A). As a result, *pMdAHA8:GUS/MdbHLH104-GFP* double
363 transgenic calli showed higher GUS activity than the *pMdAHA8:GUS* alone. However,
364 mutation of the sumoylation sites in MdbHLH104 remarkably decreased the
365 activation of the *MdAHA8* promoter (Fig. 6A). Moreover, RT-qPCR assays showed
366 that the expression levels of *MdAHA8* were noticeably induced in *MdbHLH104-GFP*
367 but not in *MdbHLH104^{K139R/K153R}-GFP* transgenic calli under the conditions of Fe
368 deficiency (Fig. 6B). Taken together, these results indicated that the sumoylation of
369 MdbHLH104 is required for its function in activating the transcription of *MdAHA8*.

370 Subsequently, WT and four transgenic calli, 35S:*MdbHLH104-GFP*
371 (*MdbHLH104-OE*), 35S:*MdbHLH104-GFP/35S:MdSIZ1-MYC*
372 (*MdbHLH104-OE/MdSIZ1-OE*), 35S:*MdbHLH104^{K139R/K153R}-GFP*
373 (*MdbHLH104^{K139R/K153R}-OE*), and 35S:*GFP* (Control), were used to assess PM
374 H⁺-ATPase-mediated acidification capacity and Fe acquisition. Under normal (pH 6)
375 conditions, there was no significant difference among the five calli. When cultivated
376 under alkaline (pH 8) conditions, however, *MdbHLH104-OE* exhibited higher PM
377 H⁺-ATPase H⁺-transport activity than the WT and control. Furthermore, it was found
378 that the promotion of PM H⁺-ATPase H⁺-transport activity was reduced when the
379 sumoylation sites of MdbHLH104 were mutated (Fig. 6C and 6D). Furthermore,
380 when *MdSIZ1* was overexpressed in *MdbHLH104* transgenic calli, the double
381 transgenic calli *MdbHLH104-OE/MdSIZ1-OE* exhibited the highest PM H⁺-ATPase
382 H⁺-transport activity (Fig. 6C and 6D), as determined by Fe content and Fe²⁺ staining

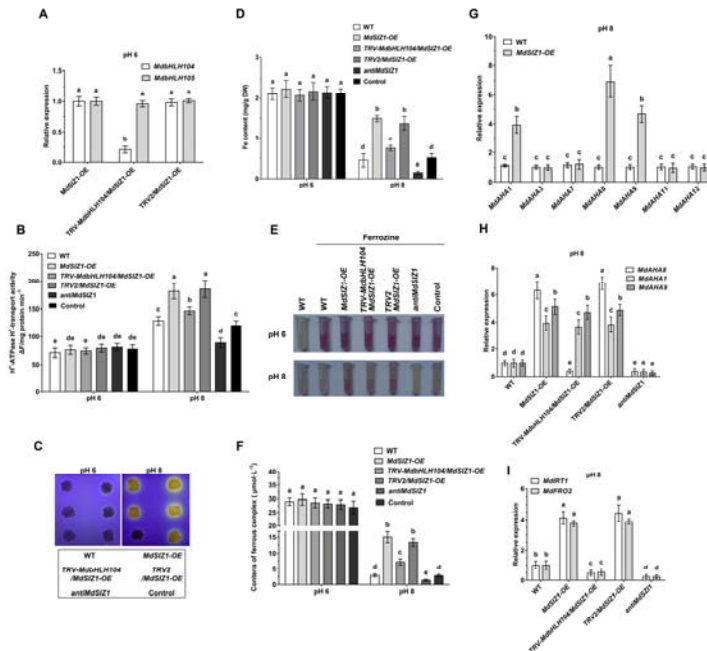


383 with Ferrozine (Fig. 6E, 6F and 6G). Taken together, these results indicated that
 384 MdbHLH104 sumoylation at residue K139 and K153 was crucial for its function in
 385 promoting PM H⁺-ATPase-mediated acidification capacity and Fe acquisition.

386 **MdSIZ1 promoted PM H⁺-ATPase-mediated acidification capacity and Fe**
 387 **homeostasis is partially MdbHLH104-dependent**

388 To further examine whether the MdSIZ1-mediated increase in PM
 389 H⁺-ATPase-mediated acidification capacity was dependent on MdbHLH104, the viral
 390 vector *TRV-MdbHLH104* was transiently transformed into *MdSIZ1-OE* transgenic
 391 calli. The empty vector *TRV2* was used as a negative control. As a result, the
 392 expression of *MdbHLH104*, but not *MdbHLH105*, was specifically inhibited in the
 393 *TRV-MdbHLH104/MdSIZ1-OE* transgenic calli (Fig. 7A).

394 Subsequently, WT and four transgenic calli, *MdSIZ1-OE* (*35S:MdSIZ1-MYC*),
 395 *TRV-MdbHLH104/MdSIZ1-OE*, *TRV2/MdSIZ1-OE*, *antiMdSIZ1* (*35S:antiMdSIZ1*),
 396 and an empty vector *35S:MYC* control were used for further investigation of PM
 397 H⁺-ATPase-mediated acidification capacity and Fe acquisition. The results showed
 398 that, under alkaline conditions, *MdSIZ1* overexpression remarkably enhanced PM
 399 H⁺-ATPase H⁺-transport activity and Fe content in transgenic calli, while its
 400 suppression decreased PM H⁺-ATPase H⁺-transport activity and Fe content (Fig. 7B,
 401 C, D, E, and F). Moreover, it was found that *MdbHLH104* suppression partially



402 abolished MdsIZ1-mediated promotion of PM H⁺-ATPase-mediated acidification
 403 capacity and Fe acquisition in *TRV-MdbHLH104/MdsIZ1-OE* transgenic calli (Fig.
 404 7B, C, D, E, and F). These results indicated that other MdaHAs may also be
 405 regulated by MdsIZ1, and MdsIZ1 promotion of PM H⁺-ATPase-mediated
 406 acidification capacity and Fe homeostasis was at least partially dependent on
 407 MdbHLH104.

408 In apple plants, 7 MdaHAs are possibly responsible for rhizosphere acidification,
 409 and MdaHA8 is directly regulated by MdbHLH104 (Zhao et al., 2016 a). None of
 410 these MdaHAs interacted with MdsIZ1 (Supplemental Fig. S8). RT-qPCR assays
 411 demonstrated that MdsIZ1 positively modulated the transcript levels of three *MdaHA*
 412 genes (*MdaHA1*, *MdaHA8*, and *MdaHA9*) (Fig. 7G). Moreover, it was found that
 413 *MdbHLH104* suppression completely abolished the MdsIZ1-mediated increase in
 414 *MdaHA8* transcripts, but not that of *MdaHA1* and *MdaHA9*. In contrast, *MdsIZ1*
 415 suppression inhibited the expression of all three genes in the *antiMdsIZ1* transgenic
 416 calli (Fig. 7H), indicating that MdsIZ1 directly regulated the expression of *MdaHA8*
 417 in an MdbHLH104-dependent manner, but it indirectly modulated the transcription of
 418 *MdaHA1* and *MdaHA9* in an MdbHLH104-independent manner.

419 The ferric reduction assays in Fig. 6F and Fig. 7E indicated that MdsIZ1 may be

420 involved in the regulation of responses downstream of ferric reduction, such as those
421 mediated by FIT and the Ib subgroup bHLH transcription factors. In apple, it was
422 found that *MdbHLH104* directly binds to the promoters of two Ib subgroup bHLH
423 genes, *MdbHLH38* and *MdbHLH39* (Zhao et al., 2016 a). We thus detected the
424 transcript levels of *MdbHLH38* and *MdbHLH39* in the WT, *MdbHLH104-OE*,
425 *MdSIZ1-OE*, and *antiMdSIZ1* transgenic calli by RT-qPCR assays. The results
426 showed that *MdbHLH104* and *MdSIZ1* positively regulated *MdbHLH38* and
427 *MdbHLH39* expression in pH 8 conditions (Supplemental Fig. S9), indicating that
428 sumoylation of *MdbHLH104* mediated by *MdSIZ1* promoted the ferric reduction
429 processes in apple in part through *MdbHLH38* and *MdbHLH39*.

430 Subsequently, the transcript levels of *MdFRO2* and *MdIRT1*, which play crucial
431 roles in Fe^{3+} reduction and Fe^{2+} absorption, were detected by RT-qPCR assays. It was
432 found that *MdbHLH104* suppression partially abolished the *MdSIZ1*-mediated
433 increase in *MdFRO2* and *MdIRT1* transcripts. In contrast, *MdSIZ1* suppression
434 inhibited the expression of all genes tested in the *antiMdSIZ1* transgenic calli (Fig. 7I).
435 These results suggested that *MdSIZ1* regulated the expression of *MdFRO2* and
436 *MdIRT1*, partially dependent on *MdbHLH104*. Taken together, these observations
437 indicated that *MdSIZ1* promoted PM H^+ -ATPase-mediated acidification capacity and
438 Fe homeostasis by partially depending on *MdbHLH104*.

439
440

441 **Discussion**

442 Plants undergo various abiotic stresses during growth and development. Among the
443 E3 ligase enzymes involved in sumoylation, SIZ1 participates in the regulation of
444 processes related to various abiotic stresses, such as phosphate starvation, low
445 temperature, drought, and ABA, via direct modification of target proteins (Miura et al.
446 2005, 2007; Catala et al. 2007; Zheng et al., 2012; Zhou et al., 2017). In addition, the
447 bHLH TF MdbHLH104 directly regulates the *MdAHA8* gene to modulate PM
448 H⁺-ATPase-mediated rhizosphere acidification and Fe homeostasis (Zhao et al., 2016
449 a). Here, it was found that the apple SUMO E3 ligase MdSIZ1 interacted with and
450 sumoylated MdbHLH104, thereby promoting PM H⁺-ATPase-mediated rhizosphere
451 acidification and regulating Fe homeostasis.

452 In most cases, SIZ1-mediated sumoylation of target proteins occurs at only one
453 site, which contains the consensus sequence ϕ -K-X-E/D (Sampson et al. 2001). For
454 example, *Arabidopsis* SIZ1 sumoylates the MYB30, ICE1, and COP1 proteins at their
455 K283, K393, and K193 residues, respectively (Miura et al., 2007; Zheng et al., 2012;
456 Lin et al., 2016). In this study, however, it was found that MdSIZ1 sumoylated
457 MdbHLH104 at two residues, K139 and K153 (Fig. 4). These two sumoylation sites
458 are highly conserved among bHLH104 homologues in both dicotyledonous and
459 graminaceous plants (Supplemental Fig. 4), suggesting a novel sumoylation pattern
460 for MdbHLH104 in plants.

461 According to previous studies, in contrast to ubiquitination, in which the substrate
462 proteins were recognized by and interacted with various E3 ligases, a single E2
463 recognizes the sumoylation site consensus sequence ϕ -K-X-E/D and E3 recognizes
464 additional target proteins in sumoylation (Sampson et al., 2001; Flotho and Melchior,
465 2013). During the sumoylation process, the E3 ligase enzyme binds to the E2
466 conjugating enzyme and promotes the transfer of SUMO to the target proteins (Gill,
467 2004). In this study, a bHLH TF, MdbHLH104, was identified as a direct target
468 protein of SUMO E3 ligase MdSIZ1 and mutation of sumoylation sites inhibited the
469 SUMO modification of MdbHLH104 by MdSIZ1. These results suggest that in the
470 process of sumoylation of MdbHLH104, the E3 ligase MdSIZ1 locks the flexible

471 SUMO~MdSCE1 thioester bond in an orientation that is favourable for nucleophilic
472 attack by the target lysine.

473 In plants, the HLH region of bHLH TFs facilitates the formation of homodimers
474 and/or heterodimers, which may play a critical role in the determination of gene
475 function (Leivar et al., 2008). In Arabidopsis, bHLH104 interacts with bHLH105 to
476 modulate Fe homeostasis (Zhang et al., 2015). The proteins bHLH104, bHLH34, and
477 bHLH105 form heterodimers or homodimers to up-regulate the expression of
478 *bHLH38/39/100/101* and *PYE*, thereby regulating Fe homeostasis (Li et al., 2016).
479 Most recently, it was reported that apple MdbHLH104 forms heterodimers with other
480 IVc subgroup bHLH TFs to activate the transcription of the PM H⁺-ATPase gene
481 *MdAHA8* (Zhao et al., 2016 a). In this study, it was found that MdSIZ1 specifically
482 interacted with and sumoylated MdbHLH104. Thus, MdbHLH104 may play a key
483 role in the IVc subgroup bHLH complex during the MdSIZ1-mediated regulation of
484 PM H⁺-ATPase activity and Fe homeostasis. Moreover, in addition to *MdAHA8*, the
485 direct target of MdbHLH104, MdSIZ1 also transcriptionally modulated the expression
486 of *MdAHA1* and *MdAHA9* (Fig. 7G), suggesting that MdSIZ1 likely targets other TFs
487 responsible for the transcriptional activity of these genes.

488 Based on our data, FIT-dependent ferric reduction was activated by MdSIZ1 and
489 MdbHLH104 under Fe deficiency (Fig. 6F and Fig 7E). These results suggest that the
490 sumoylation of MdbHLH104 by MdSIZ1 could induce Ib subgroup bHLH proteins.
491 In Arabidopsis, bHLH104 and bHLH105 formed a heterodimer to bind directly to the
492 promoters of Ib subgroup bHLH genes such as *bHLH38*, *bHLH39*, *bHLH100* and
493 *bHLH101* (Zhang et al., 2015). FIT interacts with bHLH38/39/100/101 to activate the
494 expression of *IRT1* and *FRO2* (Li et al., 2016). In apple, there are four Ib subgroup
495 bHLH TF members. Among them, MdbHLH104 directly binds to the promoters of
496 two Ib subgroup bHLH genes, *MdbHLH38* and *MdbHLH39* (Zhao et al., 2016 a).
497 RT-qPCR assays showed that the transcript levels of *MdbHLH38* and *MdbHLH39*
498 were efficiently up-regulated by MdbHLH104 and MdSIZ1 under the conditions of
499 Fe deficiency (Supplemental Fig. S9). The sumoylation of MdbHLH104 could
500 promote the expression of *MdbHLH38* and *MdbHLH39*, and thus activate the

501 *MdFRO2* and *MdIRT1* gene.

502 A previous study showed that only *MdbHLH38* and *MdbHLH39* were regulated
503 by *MdbHLH104* (Zhao et al., 2016 a). Given that suppression of *MdbHLH104* in the
504 *MdSIZ1-OE* background did not completely abolish the *MdSIZ1*-mediated increase in
505 *MdFRO2* and *MdIRT1* transcripts (Fig. 7I), we suspect that *MdSIZ1* may regulate
506 other Ib subgroup bHLH TFs in an *MdbHLH104*-independent manner. These results
507 suggest that *MdSIZ1* serves a global role in regulating Fe homeostasis in plants.

508 Sumoylation of target proteins in plants is carried out by three enzymatic steps,
509 similar to the ubiquitination pathway. These steps involve the heterodimeric activating
510 enzyme E1 (SAE1 and SAE2), a single E2 conjugating enzyme called SCE1, and two
511 classes of E3 ligase enzymes, including MMS21 and SIZ1 (Miura et al. 2005; Huang
512 et al. 2009; Ishida et al. 2012; Novatchkova et al. 2012). During the sumoylation
513 process, the E3 ligase enzyme binds to the E2 conjugating enzyme and promotes the
514 transfer of SUMO to the target proteins (Gill, 2004). In apples, both *MdSCE1* and
515 *MdSIZ1* were transcriptionally induced by Fe deficiency, and *MdSIZ1* overexpression
516 did not influence the transcript level of *MdSCE1* (Supplemental Fig. S10). Thus, the
517 E2 conjugating enzyme *MdSCE1* became a limiting factor when *MdSIZ1* was
518 overexpressed under conditions of Fe sufficiency. This underlies why
519 *MdSIZ1*-mediated sumoylation of the *MdbHLH104* protein and promotion of PM
520 H⁺-ATPase-mediated acidification capacity occurs only under Fe-deficiency
521 conditions, but not in response to Fe sufficiency, in both plants and calli (Fig. 2B-2G;
522 Supplemental Fig. 2C-2F).

523 Heterologous expression of *MdSIZ1*, an apple SUMO E3 ligase, enhanced PM
524 H⁺-ATPase-mediated rhizosphere acidification and Fe uptake in *Arabidopsis* (Fig. 2),
525 suggesting that the SIZ1-bHLH104-AHA regulatory module and pathway are
526 conserved in plants. In addition to Fe deficiency, PM H⁺-ATPases are involved in the
527 responses to various abiotic stresses in plants. In *Medicago Sativa*, AHA3
528 protein levels and H⁺-ATPase activity are positively induced by salt stress (Siboleet
529 al., 2005). In addition, the soybean (*Glycine max*) PM H⁺-ATPase gene (Gene
530 accession number AF091303) is transcriptionally induced by Aluminum (Al)

531 treatment (Shen et al., 2005). Recently, it has also been reported that the Arabidopsis
532 PM H⁺-ATPases AHA2 and AHA7 play an important role in H⁺ efflux at the root tip
533 in response to low-phosphorus stress (Yuan et al., 2017). For the mechanism of
534 SIZ1-mediated sumoylation in regulating plants tolerance to abiotic stresses, most
535 studies have focused on the mechanism of its direct regulation of target proteins
536 related to stresses. For example, SIZ1 targets PHR1 proteins for SUMO modification
537 to regulate the phosphate deficiency response (Miura et al., 2005). On the other hand,
538 SIZ1-mediated sumoylation may also affect plant tolerance to abiotic stresses via
539 regulating PM H⁺-ATPase activity. Therefore, the conserved SIZ1-bHLH104-AHA
540 regulatory module and pathway in plants serve in abiotic stress resistance processes
541 beyond their role in Fe homeostasis in apple.

542 Fe is a crucial micronutrient in plants. Both Fe overload and deficiency limit
543 plant growth and development and decrease crop yield and quality, often resulting in
544 death of the plants (Briat et al., 2015; Pinto et al., 2016). Therefore, plants have
545 evolved sophisticated mechanisms to maintain Fe homeostasis (Zhang et al., 2015; Li
546 et al., 2016; Zhao et al., 2016 a; Zhao et al., 2016 b). MdbHLH104 degradation was
547 inhibited by MG132 (Fig. 5A, B and C), suggesting that MdbHLH104 degradation
548 likely occurs via a 26S proteasome pathway. In apple plants, the scaffold protein
549 MdbT2 recruits Cullin-RING ubiquitin Ligase 3 (CRL3) to form the MdbT2^{MdCUL3}
550 complex, which in turn ubiquitinates and degrades MdbHLH104 (Zhao et al., 2016 b).
551 In this study, it was found that MdSIZ1 stabilized MdbHLH104 via SUMO
552 modification, indicating that sumoylation and ubiquitination have antagonistic effects
553 on MdbHLH104. MdbT2^{MdCUL3}-mediated degradation of the MdbHLH104 protein
554 under Fe-sufficient conditions prevents injury caused by over-accumulation of Fe. On
555 the other hand, under conditions of Fe deficiency, MdbHLH104 sumoylation plays the
556 opposite role and promotes Fe uptake from the soil, indicating that different
557 post-transcriptional modifications of MdbHLH104 play distinct roles in regulating Fe
558 homeostasis. In addition to MdbHLH104, sumoylation and ubiquitination of the
559 MdMYB1 TF have antagonistic effects on anthocyanin accumulation (Li et al., 2012;
560 Zhou et al., 2017). Thus, sumoylation and ubiquitination play an important role in

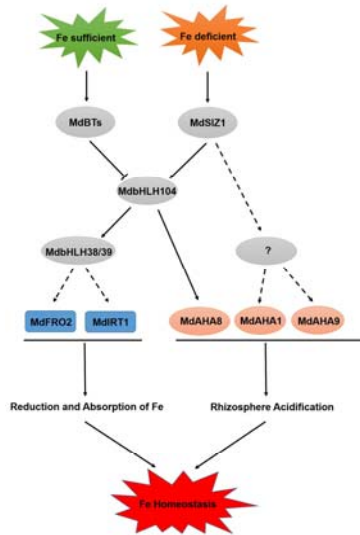
561 balancing plant responses to ambient environment signals via the modification of
562 specific target proteins.

563 Both MdBT2 and MdSIZ1 regulate MdbHLH104 (Fig. 8; Zhao et al., 2016 b). As
564 downstream targets of MdbHLH104, PM H⁺-ATPases are not only involved in Fe
565 uptake, but they also provide energy for absorption and transportation of other
566 nutrients into plant cells by generating electrochemical gradients (Haruta and
567 Sussman, 2012). In soybeans, under Al stress conditions, the phosphorylation of PM
568 H⁺-ATPases and their interaction with 14-3-3 proteins are inhibited, resulting in
569 inhibition of NO₃⁻ uptake (Yang et al., 2016). In addition, Ni uptake by wheat
570 (*Triticum aestivum*) roots partially requires increased generation of a proton gradient
571 by PM H⁺-ATPases (Dalir et al., 2017). Furthermore, PM H⁺-ATPases play an
572 important role in regulating plant growth and development, as well as in the response
573 to various stresses (Siboleet al., 2005; Shen et al., 2005; Kim et al., 2013), and both
574 BT2 and SIZ1 are expressed in response to various environmental and endogenous
575 signals (Miura et al., 2005; Mandadi et al., 2009; Zheng et al., 2012). Therefore, the
576 MdBT2/MdSIZ1-MdbHLH104-MdAHA8 regulatory module and pathway serve in
577 multiple processes beyond their role in Fe homeostasis in plants.

578

579 **Conclusions**

580 In summary, our findings provide new insights into the mechanisms by which plants
581 respond via an MdSIZ1-MdbHLH104-PM H⁺-ATPase pathway to control the Fe
582 supply status (Fig. 8). Fe deficiency induces sumoylation of the Fe
583 homeostasis-associated bHLH TF MdbHLH104 and other unknown TFs by enhancing
584 the transcript levels of the gene encoding the SUMO E3 ligase MdSIZ1. Sumoylation
585 of target proteins promotes their stability by inhibiting conjugation of ubiquitin
586 molecules. Stabilized MdbHLH104 and other TFs directly or indirectly activate the
587 transcription of genes encoding PM H⁺-ATPases, such as *MdAHA1*, *MdAHA8*, and
588 *MdAHA9*, to promote rhizosphere acidification. Meanwhile, MdSIZ1 also promotes
589 the expression of *MdbHLH38* and *MdbHLH39*, and thus activates the transcription of
590 *MdFRO2* and *MdIRT1* to convert Fe³⁺ to Fe²⁺ and import Fe²⁺ across root epidermal



591 cell membranes into the plants.

592

593 **Materials and Methods**

594 **Plant materials and growth conditions**

595 The calli of 'Orin' apples were subcultured as described by Zhao et al. (2016 a).
 596 Briefly, the calli were grown on Murashige and Skoog (MS) medium with 1.5 mg/L
 597 2,4-D (2,4-Dichlorophenoxyacetic acid) and 0.4 mg/L 6-BA (6-Benzylaminopurine)
 598 at 25 °C in the dark. The Fe-sufficient media was the MS media containing 100 µM
 599 Fe(II)-EDTA. The Fe-deficient media was the same without Fe(II)-EDTA. For
 600 alkaline treatment, MS media at a pH of 8 was used.

601 The 'Gala' apple tissue cultures were grown on MS subculture medium containing
 602 0.5 mg/L 6-BA, 0.2 mg/L NAA (1-Naphthylacetic acid), and 0.1 mg/L GA
 603 (Gibberellin) for *Agrobacterium rhizogenes*-mediated transformation and other
 604 analyses. The Fe-sufficient media was the MS media containing 100 µM Fe(II)-EDTA.
 605 The Fe deficient media was the same without Fe(II)-EDTA. For apple plants with
 606 transgenic hairy roots, sand with the addition of Hoagland's solution (Hoagland and
 607 Arnon, 1950) of pH 6 or pH 8 was used.

608 *Arabidopsis thaliana* (ecotype 'Columbia') was grown on MS medium at 22°C
 609 under a long-day photoperiod (16-h light/8-h dark). For alkaline treatment, the MS
 610 media at a pH of 8 was used.

611 **Vector construction and genetic transformation**

612 The *MdbHLH104-GFP* and *PMdAHA8:GUS* vectors were constructed as described
613 by Zhao et al. (2016 a). The *MdSIZ1-MYC* and *antiMdSIZ1* vectors were constructed
614 as described by Zhou et al. (2017). *MdbHLH104-GFP*, *MdSIZ1-MYC*, and
615 *antiMdSIZ1* were under the control of the 35S promoter. Subsequently, the resultant
616 vectors were genetically transformed into apple calli and Arabidopsis plants with the
617 *Agrobacterium tumefaciens* strains LBA4404 and GV3101, as described by Horsch et
618 al. (1985).

619 *Agrobacterium rhizogenes*-mediated transformation was performed as described
620 by Guidarelli et al. (2014) and Xiao et al. (2014) with minor modifications. Briefly, a
621 350-bp fragment of *MdSIZ1* (1197–1546 bp) was inserted into the
622 pK7GWIWG2(II)-RedRoot vector under control of the 35S promoter using Gateway
623 cloning technology to construct the RNA interference (RNAi) transformation vector.
624 The following primer pairs were used: asMdSIZ1-F/ asMdSIZ1-R for 350-bp
625 fragment of *MdSIZ1*, RNAi-MdSIZ1-F/RNAi-MdSIZ1-R for the fragment used for
626 Gateway cloning (Table S1). The resultant vector, harboring a 35S:DsRED1 cassette
627 to overexpress the DsRED fluorescent protein, was introduced into *A. rhizogenes*
628 MSU440 with the help of the pRiA4 plasmid and then used for transient
629 transformation.

630 Subsequently, 3-week-old 'Gala' apple tissue cultures were cut off a part of the
631 stem and then immersed in *A. rhizogenes* MSU440 solution ($OD_{600}=0.6-0.8$) for 15
632 min. Inoculated plants were then transferred to 1/2 MS medium containing 300 mg/L
633 cefotaxime at 25 °C for hairy root induction. Examination of transgenic hairy roots for
634 DsRED1 fluorescence was performed using a fluorescence microscope (AX10) (Carl
635 Zeiss, Germany) employing the DsRED filter set (excitation: 546/12 nm, emission:
636 605/75 nm). As a result of preliminary tests, non-transformed hairy roots lacking
637 DsRED fluorescence were cut off, and the transformed chimera plants were then used
638 for follow-up experiments.

639 **Gene expression analysis**

640 Total RNA was isolated from apple plants, hairy roots, calli, and Arabidopsis plants

641 using an OmniPlant RNA Kit (DNase I) (Cwbiotech, Beijing, China), following the
642 manufacturer's instructions. First-strand cDNA was synthesized using a PrimeScript
643 first-strand cDNA synthesis kit (Takara, Dalian, China), following the manufacturer's
644 instructions.

645 Subsequently, cDNA was diluted to 2.5 ng μl^{-1} with ddH₂O for reverse
646 transcription quantitative PCR (RT-qPCR), and the reactions were performed using
647 the UltraSYBR Mixture (with ROX I) (Cwbiotech, Beijing, China) in a reaction
648 volume of 20 μl . The following primer pairs were used: QS-F/QS-R for *MdSIZ1*,
649 Q104-F/Q104-R for *MdbHLH104*, Q105-F/Q105-R for *MdbHLH105*, QI-F/QI-R for
650 *MdIRT1*, QF-F/QF-R for *MdFRO2*, QA1-F/QA1-R for *MdAHA1*, QA3-F/QA3-R for
651 *MdAHA3*, QA7-F/QA7-R for *MdAHA7*, QA8-F/QA8-R for *MdAHA8*, QA9-F/QA9-R
652 for *MdAHA9*, QA11-F/QA11-R for *MdAHA11*, and QA12-F/QA12-R for *MdAHA12*
653 (Table S2). *Md18S* and *MdActin* were used as internal controls.

654 **Yeast two-hybrid assay**

655 Yeast (*Saccharomyces cerevisiae*) two-hybrid assays (Y2H) were performed as
656 described by Zhou et al. (2017). Briefly, full-length cDNAs of *MdSCE1*, *MdbHLH104*,
657 *MdbHLH105*, *MdbHLH115*, *MdbHLH11*, *MdbHLH121*, *MdPYE*, *MdAHA1*, *MdAHA3*,
658 *MdAHA7*, *MdAHA8*, *MdAHA9*, *MdAHA11*, and *MdAHA12* were inserted into
659 *pGAD424* (Clontech) to generate an in-frame fusion with the GAL4 activation
660 domain. The primer pairs used for gene cloning are listed in Supplemental Table S1.
661 The domain-deleted form (1-427aa) of *MdSIZ1* was excised by *SmaI* and *PstI* double
662 digestion and cloned into *pGBT9* to generate an in-frame fusion with the GAL4
663 DNA-binding domain. Full-length *MdSIZ1* was self-activated in β -galactosidase
664 assays in yeast. All of the constructs were transformed into the Y2H strain using the
665 lithium acetate method. Subsequently, yeast cells were plated onto selective medium
666 lacking Trp and Leu (-Trp/-Leu) and the colonies were then cultured in YPDA liquid
667 medium consisting of 2% (w/v) Bacto Pepton, 1% (w/v) Yeast extract, 2% (w/v)
668 Glucose, and 1% (v/v) 100x Adenine until OD₆₀₀ reached 0.25. Next, the solution was
669 diluted 10 times, 100 times and 1000 times in turn and dropped on the selective
670 medium lacking Trp and Leu (-Trp/-Leu), or lacking Trp, Leu, His, and Adenine

671 (-Leu/-Trp/-His/-Ade), and grown for 2 days at 28 °C.

672 **Pull-down assays**

673 These assays were performed as described by Zhou et al. (2017). The *MdbHLH104*
674 coding sequence was amplified using the primer pair MdbHLH104-F/MdbHLH104-R
675 (Table S1) and excised by *BamHI* and *Sall* double digestion and then cloned into the
676 *PGEX-4T-1* vector for GST-tag fusion. The full-length cDNA of *MdsIZ1* was
677 amplified using the primer pair MdsIZ1-F/MdsIZ1-R (Table S1) and cloned into the
678 *pEASY-Blunt E1* expression vector using original TA cloning kit (Transgene, Beijing,
679 China) for His-tag fusion. Then, both proteins were individually expressed in and
680 purified from *Escherichia coli* BL21 (DE3). Subsequently, recombinant
681 GST-MdbHLH104 fusion and His-MdsIZ1 fusion proteins were mixed in equal
682 volumes, and following incubation, were purified with a GST column. The pellet
683 fraction was then detected via immunoblotting using an anti-His antibody (Abmart,
684 Shanghai, China).

685 **Co-IP assay**

686 For co-immunoprecipitation (Co-IP) assays, MdbHLH104-GFP and GFP proteins
687 were IPed from the *35S:MdbHLH104-GFP* and *35S:GFP* (pBIN) transgenic apple
688 plants with anti-GFP antibodies (Abmart, Shanghai, China) using the Pierce classic IP
689 kit (Thermo, Shanghai, China), following the manufacturer's instructions.
690 MdbHLH104-GFP proteins and GFP proteins in whole-cell lysates (Input) and
691 MdsIZ1 proteins in the pellet fraction (IP) were detected via immunoblot analysis
692 with anti-GFP and anti-MdsIZ1 antibodies (Customized by Abmart, Shanghai, China),
693 respectively.

694 **Sumoylation assays**

695 Sumoylation assays were performed *in vivo* as described by Zhou et al. (2017).
696 Briefly, 6 µg of GST-MdbHLH104, GST-MdbHLH104^{K139R}, GST-MdbHLH104^{K153R},
697 and GST-MdbHLH104^{K139R/K153R} were incubated with 0.5 µg of recombinant human
698 SAE1 protein (Product code: ab96772), 0.5 µg of SAE2/UBA2 peptide (Product code:
699 ab109093), 2 µg of human UBE2I / UBC9 peptide (Product code: ab30701), 5 µg of
700 recombinant human SUMO1 protein (Product code: ab3801) (Abcam, Cambridge,

701 UK), and with or without 8 µg of His-MdsIZ1 for 1.5 h at 37 °C. Sumoylated proteins
702 were double detected with anti-SUMO1 (Abcam, Cambridge, UK) and anti-GST
703 antibodies (Abmart, Shanghai, China), respectively.

704 For *in vivo* sumoylation assays, the 28-day-old *MdbHLH104-GFP* transgenic
705 apple plants and 2-week-old transgenic calli overexpressing the *MdbHLH104-GFP*,
706 *MdbHLH104-GFP/MdsIZ1-MYC*, *MdbHLH104-GFP/antiMdsIZ1*, or
707 *MdbHLH104^{K139R/K153R}-GFP* fusions were treated in Fe-deficiency conditions for 1 h
708 before total proteins were immunoprecipitated with anti-GFP antibodies using a
709 Pierce classic IP kit (Thermo, Shanghai, China), following the manufacturer's
710 instructions. Western blot analyses were subsequently performed with anti-GFP
711 (Abmart, Shanghai, China) or anti-SUMO1 (Abmart, Shanghai, China) antibodies.

712 **Protein degradation assays**

713 For *in vivo* degradation assays, after pretreatment in Fe deficient conditions for 1 h,
714 2-week-old *MdbHLH104-GFP*, *MdbHLH104-GFP/MdsIZ1-MYC*,
715 *MdbHLH104^{K139R/K153R}-GFP*, and *MdbHLH104^{K139R/K153R}-GFP/MdsIZ1-MYC*
716 transgenic calli were placed in Fe-sufficient liquid medium containing 250 µM
717 cycloheximide (CHX) translational inhibitor for different durations and sampled
718 simultaneously to detect *MdbHLH104-GFP* protein abundance using an anti-GFP
719 antibody. For MG132 (26S proteasome inhibitor) treatment, the Fe deficiency
720 pretreated transgenic calli were treated with 50 µM MG132 for 6 h and then used for
721 the protein degradation assay. DMSO was used as a negative control for MG132. The
722 protein concentrations were quantified using Quantity One 1-D Analysis Software
723 (Bio-Rad, USA).

724 ***In vivo* ubiquitination assays**

725 For the *in vivo* ubiquitination assays, the Fe deficiency pretreated transgenic calli
726 overexpressing *MdbHLH104-GFP*, *MdbHLH104-GFP/MdsIZ1-MYC*, and
727 *MdbHLH104^{K139R/K153R}-GFP* were treated with 50 µM MG132 for 6 h and then treated
728 with Fe sufficient conditions for 6 h or not. Then, *MdbHLH104-GFP* proteins were
729 IPed using an anti-GFP antibody using the Pierce classic IP kit (Thermo, Shanghai,
730 China), following the manufacturer's instructions. *MdbHLH104-GFP* proteins in

731 whole-cell lysates prior to treatment (Input) and in the pellet fraction (IP), or
732 ubiquitinated MdbHLH104 proteins in the pellet fraction (IP), were detected via
733 immunoblot analysis with anti-GFP and anti-ubiquitin antibodies (Sigma-Aldrich,
734 Germany), respectively.

735 **Viral vector-based transformation analysis**

736 To generate antisense viral expression vectors, the *MdbHLH104* fragment was
737 amplified using the primer pair asMdbHLH104-F/asMdbHLH104-R (Table S1) and
738 excised by *EcoRI* and *KpnI* double digestion and then cloned into the *tobacco rattle*
739 *virus* (TRV) vector in the antisense orientation under the control of the dual 35S
740 promoter. The resultant vectors were then transiently transformed into *MdSIZ1-MYC*
741 transgenic calli using the *Agrobacterium tumefaciens* strain LBA4404 with the
742 auxiliary vector *TRV1*. The empty vector *TRV2* was used as a negative control.

743 **PM H⁺-ATPase H⁺-transport activity assays**

744 Plasma membrane H⁺-ATPases were isolated as described by Zhao et al. (2016 a). The
745 apple calli were grown on Fe-sufficient normal media and then transferred to the
746 media at a pH of 6 or 8 for 5 days for PM H⁺-ATPase H⁺-transport activity detection.
747 For *Agrobacterium tumefaciens*-infected apple plants, the plants with transgenic roots
748 were grown on sand with the addition of Hoagland's solution of pH 6 for 1 month, and
749 then transferred to the sand with the addition of Hoagland's solution of pH 6 or pH 8
750 for 7 days for PM H⁺-ATPase H⁺-transport activity detection. For Arabidopsis, the
751 14-day-old seedlings grown on normal (pH 6) or alkaline (pH 8) media were used.
752 Plasma membranes were isolated with a buffer consisting of 15 mM Tris-Cl (pH 7.5),
753 0.5 M sucrose, 1 mM EGTA, 1 mM EDTA, 6% (w/v) PVP, 0.1% (w/v) BSA, 0.1 mM
754 DTT and 1 mM PMSF. Microsomal pellets were obtained from the homogenate as
755 described by Zhao et al. (2016 a). All steps were performed at 4 °C or on ice.
756 Subsequently, an inside-acid pH gradient (Δ pH), which was formed in the vesicles by
757 the activity of the H⁺-ATPase, was measured as a decrease (quench) in the
758 fluorescence of quinacrine (a pH-sensitive fluorescent probe), which has been
759 described in detail by Zhao et al. (2016 a). Specific PM H⁺-ATPase H⁺-transport
760 activity was calculated by dividing the change in fluorescence by the mass of PM

761 protein in the reaction per unit time ($\Delta F/\text{min}$ per mg of protein).

762 **GUS analysis**

763 Histochemical staining to detect GUS activity and quantitative analysis of GUS in
764 apple calli was performed as described by Xie et al. (2012).

765 For histochemical staining, the transgenic calli were immersed in GUS staining
766 buffer (1 mM 5-bromo-4-chloro-3-indolyl- β -glucuronic acid solution in 100 mM
767 sodium phosphate pH 7.0, 0.1 mM EDTA, 0.5 mM ferrocyanide, 0.5 mM ferricyanide,
768 and 0.1% (v/v) Triton X-100) at 37°C for 1 h. After staining, the calli were
769 photographed.

770 For the quantitative analysis of GUS activity, the proteins were extracted with 1
771 ml of extraction buffer (50 mM NaHPO₄ PH 7.0, 10 mM β -mercaptoethanol, 10 mM
772 Na₂EDTA, 0.1% (v/v) Triton X-100) and 1 ml RIPA Lysis Buffer (Beyotime, Beijing,
773 China) from the transgenic apple calli. The concentration of total protein was
774 determined with the Protein Assay kit (Bio-Rad, USA). One hundred milliliters of the
775 extract was then added to 900 μ L of GUS reaction buffer containing 1 mM
776 4-methylumbelliferone glucuronide (4-MUG), and the mixture was incubated at 37°C.
777 After the reaction proceeded for 0, 5, 10, 15, 30, and 60 min, 100 μ l of the reaction
778 mixture was added to 900 μ l of the stop solution (1 M sodium carbonate). The
779 fluorescence was measured using a Versa Flour Spectrofluorometer at an excitation
780 wavelength of 365 nm and an emission wavelength of 450 nm.

781 **Chlorophyll content measurement**

782 The *Agrobacterium tumefaciens*-infected apple plants were grown on sand with the
783 addition of Hoagland's solution of pH 6 for 1 month, and then transferred to the sand
784 with the addition of Hoagland's solution of pH 6 or pH 8 for 20 days. Subsequently,
785 the young leaves were collected and ground into powder in liquid nitrogen to measure
786 chlorophyll content. The powder was then resuspended in 80% (v/v) acetone and
787 centrifuged at 10,000 g for 5 min. Chlorophyll concentrations were calculated as
788 described by Zhao et al. (2016 a). For Arabidopsis, the 14-day-old seedlings grown on
789 normal (pH 6) or alkaline (pH 8) media were used.

790 **Rhizosphere acidification assay**

791 Acidification assays were performed as described by Yi et al. (1994) and Zhao et
792 al. (2016 a). The apple calli were grown on normal medium (pH 6) for 14 days,
793 transferred to alkaline medium (pH 8) for 5 days, and then transferred to 1% (w/v)
794 agar plates containing 0.006% (w/v) bromocresol purple and 0.2 mM CaSO₄ (pH
795 6.0-6.5) for 36 h for phenotype analysis.

796 For *Agrobacterium tumefaciens*-infected apple plants, the plants were grown on
797 sand with the addition of Hoagland's solution of pH 6 for 1 month, and then
798 transferred to the sand with the addition of Hoagland's solution of pH 6 or pH 8 for 7
799 days. Subsequently, the plants were transferred to a 1% (w/v) agar plate containing
800 0.006% (w/v) bromocresol purple and 0.2 mM CaSO₄ (pH 6.0-6.5) for 36 h for
801 phenotype analysis.

802 For *Arabidopsis*, seeds were germinated on normal (pH 6) or alkaline medium
803 (pH 8) for 14 days. Subsequently, three plants of every line were transferred to
804 bromocresol purple agar plates, as mentioned above, for 36 h for phenotype analysis.

805 **Ferrous staining assay**

806 The apple calli were grown on normal medium (pH 6) for 14 days, and then
807 transferred to alkaline medium (pH 8) for 5 days. Subsequently, the calli were
808 transferred to liquid MS media containing 300 μM Ferrozine for 12 h for ferrous
809 staining. Ferrozine reagent forms a red-colored complex with ferrous iron, but not
810 with ferric iron, and the Fe(II) is trapped by Ferrozine to produce a red product
811 (Stookey, 1970).

812 For quantification of ferrous complex formed by ferrozine, the optical density
813 (OD) of the complex was measured at 562 nm wavelength. At this wavelength, the
814 molar absorptivity is 27,900 (Stookey, 1970) and the concentration of the complex
815 was calculated according to Lambert-Beer law.

816 **Fe concentration measurement**

817 Fe content measurements were carried out as described by Kobayashi et al.
818 (2013). The apple calli were grown on Fe-sufficient normal media and then
819 transferred to the media at a pH of 6 or 8 for 5 days for Fe content measurement. For
820 *Agrobacterium tumefaciens*-infected apple plants, the plants with transgenic roots

821 were grown on sand with the addition of Hoagland's solution of pH 6 for 1 month, and
822 then transferred to the sand with the addition of Hoagland's solution of pH 6 or pH 8
823 for 20 days for Fe content measurement. For Arabidopsis, the 14-day-old seedlings
824 grown on normal (pH 6) or alkaline (pH 8) media were used. Apple calli, plants, and
825 Arabidopsis plants were dried for 1-2 days at 80 °C and then wet-ashed with HNO₃
826 and H₂O₂ for 60 min at 220 °C using a muffle furnace. Fe content analysis was
827 performed using inductively coupled plasma spectroscopy.

828 **Accession numbers**

829 Sequence data from this article can be found in the Genome Database for Rosacea
830 (GDR) under accession numbers: MdSIZ1 (MDP0000125173), MdSCE1
831 (MDP0000465760), MdbHLH104 (MDP0000825749), MdbHLH105
832 (MDP0000264803), MdbHLH115 (MDP0000323291), MdbHLH11
833 (MDP0000275635), MdbHLH121 (MDP0000494181), MdPYE (MDP0000301871),
834 MdAHA1 (MDP0000136397), MdAHA3 (MDP0000150049), MdAHA7
835 (MDP0000162032), MdAHA8 (MDP0000181085), MdAHA9 (MDP0000195785),
836 MdAHA11 (MDP0000249645), MdAHA12 (MDP0000259837), MdFRO2
837 (MDP0000226559), and MdIRT1 (MDP0000940721).

838

839 **Supplemental materials**

840 **Supplemental Figure S1.** MdSIZ1 is an important protein in the response to Fe
841 deficiency in apple.

842 **Supplemental Figure S2.** The transcript levels of *MdSIZ1* were inhibited in
843 transgenic hair roots of *MdSIZ1*-RNAi chimeric plants.

844 **Supplemental Figure S3.** MdSIZ1 promotes PM H⁺-ATPase-mediated acidification
845 capacity and Fe acquisition in apple calli.

846 **Supplemental Figure S4.** MdSIZ1 specifically interacts with MdbHLH104 in yeast
847 cells.

848 **Supplemental Figure S5.** Potential sumoylation site consensus sequences predicted
849 in MdbHLH104 proteins.

850 **Supplemental Figure S6.** Identification of transgenic apple calli.

851 **Supplemental Figure S7.** The transcript levels of *MdbHLH104* were not influenced
852 by MdSIZ1.

853 **Supplemental Figure S8.** Interactions among MdSIZ1 and 7 MdAHA proteins.

854 **Supplemental Figure S9.** The transcript levels of *MdbHLH38* and *MdbHLH39* were
855 up-regulated by MdbHLH104 and MdSIZ1.

856 **Supplemental Figure S10.** The expression levels of *MdSCE1*.

857 **Supplemental Table S1.** Primers used for gene cloning.

858 **Supplemental Table S2.** Primers used for RT-qPCR.

859

860 **Acknowledgements**

861 This work was financially supported by grants from the National Natural Science
862 Foundation of China (31430074 and 31772275), the Ministry of Education of China
863 (IRT15R42), the Ministry of Agriculture of China (CARS-28) and Shandong Province
864 (SDAIT-06-03).

865

866 **Figure Legends**

867 Figure 1. *MdSIZ1* knockdown increases the sensitivity of apple to Fe deficiency. After
868 28 days of subculture, ‘Gala’ apple cultures were infected with *Agrobacterium*
869 *tumefaciens* containing empty vector (Control) or *MdSIZ1*-RNAi silencing vector to
870 induce hair root. Thereinto, the infection of *MdSIZ1*-RNAi was carried out twice, and
871 each batch of 15 cultures was denoted as #1 and #2 respectively. Each batch of 15
872 cultures were randomly divided into 5 groups to conduct different experiments.
873 Biological replicates were carried out with the 3 cultures in each group to calculate
874 the standard deviation (SD), which are indicated by error bars. Different letter codes
875 have significant difference ($p < 0.01$, ANOVA, Tukey correction). A. The appearance
876 of chlorosis and total chlorophyll contents in young leaves of control and
877 *MdSIZ1*-RNAi chimeric plants in normal (pH 6) or alkaline (pH 8) medium for 20
878 days. B and C. Total Fe content in shoots and roots of control and *MdSIZ1*-RNAi
879 chimeric plants grown in normal (pH 6) or alkaline (pH 8) medium for 20 days. DW:
880 dry weight. D. PM H⁺-ATPase H⁺-transport activity in control and *MdSIZ1*-RNAi
881 chimeric plants grown in normal (pH 6) or alkaline (pH 8) medium for 7 days. E. The

882 rhizosphere acidification of control and *MdSIZ1*-RNAi chimeric plants grown in
883 normal (pH 6) or alkaline (pH 8) medium for 7 days. The yellow colour around the
884 roots stained with bromocresol purple indicates rhizosphere acidification.

885 Figure 2. Heterologous expression of *MdSIZ1* enhances Fe-deficient stress
886 tolerance in Arabidopsis seedlings. A. *MdSIZ1* expression in WT and transgenic
887 Arabidopsis seedlings. RNA was prepared from seedlings. B. Phenotypes of the WT
888 and *MdSIZ1* overexpression lines grown for 14 days on normal (pH 6) or alkaline (pH
889 8) media. Scale bars = 1 cm. C. Chlorophyll contents in 14-day-old WT and the
890 *MdSIZ1* overexpression lines. FW: fresh weight. D and E. Fe contents in 14-day-old
891 roots and shoots of plants. DW, dry weight. F. PM H⁺-ATPase H⁺-transport activity in
892 14-day-old WT and the *MdSIZ1* overexpression lines. G. Rhizosphere acidification in
893 14-day-old WT and *MdSIZ1* overexpression lines. Acidification is indicated by a
894 yellow color around the roots. Scale bars = 1 cm. Error bars indicate the SD for three
895 biological replicates in which the experiments were carried out three times using the
896 seedlings of each line. Samples denoted by different letters are significantly different
897 ($p < 0.01$, ANOVA, Tukey correction).

898 Figure 3. *MdSIZ1* interacts with *MdbHLH104* both *in vitro* and *in vivo*. A.
899 Interaction between *MdSIZ1* and *MdbHLH104* in yeast cells. Dilution series of yeast
900 cells co-expressing the indicated proteins were grown for 2 days at 28 °C. SD/-T/-L
901 indicates Leu and Trp dropout synthetic dropout medium; SD/-T/-L/-H/-A indicates
902 Leu, Trp, His, and Ade dropout synthetic dropout medium. AD-*MdSCE1* (SUMO E2
903 conjugating enzyme1) + BD-*MdSIZ1* and AD (pGAD empty vector) + BD-*MdSIZ1*
904 were used as positive and negative controls, respectively. B. Interaction between
905 *MdSIZ1* and *MdbHLH104* in an *in vitro* pull-down assay. Recombinant
906 GST-*MdbHLH104* fusion and His-*MdSIZ1* fusion proteins were mixed in equal
907 volume, and following incubation proteins were purified with a GST column. *In*
908 *vitro*-translated GST protein was used as a negative control. ‘Input’ indicates protein
909 mixtures before the experiments, ‘Pull-down’ indicates purified protein mixture. ‘+’
910 indicates presence, and ‘-’ indicates absence. IB: Immunoblot. C. Interaction between
911 *MdSIZ1* and *MdbHLH104* in a Co-IP assay. *MdbHLH104*-GFP and GFP proteins
912 were IPed from the *35S:MdbHLH104-GFP* and *35S:GFP* (pBIN) transgenic apple
913 plants with anti-GFP antibodies. *MdbHLH104*-GFP proteins and GFP proteins in
914 whole-cell lysates (Input) and *MdSIZ1* proteins in the pellet fraction (IP) were
915 detected via immunoblot analysis with anti-GFP and anti-*MdSIZ1* antibodies,

916 respectively. IB: Immunoblot. D. Interaction between MdSIZ1 and MdbHLH104 in a
917 BiFC assay. The MdSIZ1-nYFP and MdbHLH104-cYFP constructs were
918 co-expressed transiently in tobacco leaves and visualized by fluorescence microscopy.
919 DAPI was used to stain the nuclei. YFP: Yellow fluorescent protein. BF: Bright field.
920 Scale bars = 1 μ m.

921 Figure 4. MdSIZ1 directly sumoylates MdbHLH104 proteins at residues K139
922 and K153 under conditions of Fe deficiency. A. SUMO1-MdbHLH104 conjugate
923 detection *in vitro*. Free SUMO (including monomeric and polymeric forms) are
924 indicated by a brace. IB: Immunoblot. B. SUMO modification of MdbHLH104 under
925 Fe deficiency. The proteins were IPed from *35S:MdbHLH104-GFP* transgenic apple
926 plants using anti-GFP antibodies after treatment with Fe-sufficient or deficient
927 conditions for 1 h. MdbHLH104-GFP proteins in whole-cell lysates prior to treatment
928 (Input) and in the pellet fraction (IP), or sumoylated MdbHLH104 proteins in the
929 pellet fraction (IP), were detected via immunoblot analysis with anti-GFP and
930 anti-SUMO1 antibodies, respectively. IB: Immunoblot. C. Sumoylation of WT and
931 mutant MdbHLH104 proteins under conditions of Fe deficiency *in vivo*. The proteins
932 from different transgenic calli, specifically *MdbHLH104-GFP*,
933 *MdbHLH104^{K139R/K153R}-GFP*, *MdbHLH104-GFP/MdSIZ1-MYC*, and
934 *MdbHLH104-GFP/antiMdSIZ1*, were IPed with anti-GFP antibodies after treatment at
935 Fe-deficient conditions for 1 h. MdbHLH104-GFP proteins in whole-cell lysates prior
936 to treatment (Input) and in the pellet fraction (IP), or sumoylated MdbHLH104
937 proteins in the pellet fraction (IP), were detected via immunoblot analysis with
938 anti-GFP and anti-SUMO1 antibodies, respectively. MdSIZ1 proteins in whole-cell
939 lysates prior to treatment (Input) were detected by anti-MdSIZ1 antibodies to confirm
940 the transgenic calli. IB: Immunoblot.

941 Figure 5. MdSIZ1 stabilizes MdbHLH104 and inhibits its ubiquitination. A.
942 MdbHLH104 protein degradation assay *in vivo*. After pretreatment in Fe-deficient
943 conditions for 1 h, four transgenic calli, *MdbHLH104-GFP*,
944 *MdbHLH104-GFP/MdSIZ1-MYC*, *MdbHLH104^{K139R/K153R}-GFP*, and
945 *MdbHLH104^{K139R/K153R}-GFP/MdSIZ1-MYC* were placed in the Fe-sufficient fluid
946 medium containing 250 μ M translational inhibitor cycloheximide (CHX) for different
947 durations and sampled simultaneously to detect MdbHLH104-GFP protein abundance
948 using an anti-GFP antibody. For MG132 (26S proteasome inhibitor) treatment, the Fe
949 deficiency pretreated transgenic calli were treated with 50 μ M MG132 for 6 h and

950 then used for protein degradation assay. ACTIN in total protein extracts was used as a
951 loading control. DMSO was used as a negative control for MG132. B. Quantification
952 of MdbHLH104-GFP protein levels using Quantity One software (Bio-Rad, USA).
953 The protein degradation assay in A was carried out three times and the protein
954 quantities relative to the levels at initial time 0 were counted and used to calculate the
955 standard deviation (SD), as indicated by the error bars. Samples denoted by different
956 letters are significantly different ($p < 0.01$, ANOVA, Tukey correction). C and D.
957 Ubiquitination of MdbHLH104-GFP proteins in *MdbHLH104-GFP*,
958 *MdbHLH104-GFP/MdSIZ1-MYC*, and *MdbHLH104^{K139R/K153R}-GFP* transgenic calli
959 under Fe-sufficient or Fe-deficient conditions. The Fe deficiency pretreated transgenic
960 calli were treated with 50 μ M MG132 for 6 h and then treated in Fe-sufficient
961 conditions for 6 h or not. Then, MdbHLH104-GFP proteins were IPed using an
962 anti-GFP antibody. MdbHLH104-GFP proteins in whole-cell lysates prior to treatment
963 (Input) and in the pellet fraction (IP), or ubiquitinated MdbHLH104 proteins in the
964 pellet fraction (IP), were detected via immunoblot analysis with anti-GFP and
965 anti-ubiquitin antibodies, respectively. The sumoylated MdbHLH104 proteins in the
966 pellet fraction (IP) were detected by anti-SUMO1 antibodies. Asterisks indicate
967 sumoylated MdbHLH104 bands. IB: Immunoblot.

968 Figure 6. MdbHLH104 sumoylation at residues K139 and K153 is crucial for its
969 function in activating *MdAHA8* transcription and promoting Fe acquisition. A.
970 Promoter activity assays using GUS staining and GUS activity assays. The
971 2-week-old transgenic calli were treated in Fe-deficient conditions for 5 days and then
972 used for GUS staining and GUS activity measurements. B. *MdAHA8* expression as
973 measured by RT-qPCR in WT, *MdbHLH104-OE*, and *MdbHLH104^{K139R/K153R}-OE*
974 transgenic calli under Fe-sufficient or deficient conditions respectively. C. PM
975 H⁺-ATPase H⁺-transport activity of WT, *MdbHLH104-OE/MdSIZ1-OE*,
976 *MdbHLH104-OE*, *MdbHLH104^{K139R/K153R}-OE*, and Control (*35S:GFP*) transgenic
977 apple calli. The 2-week-old transgenic calli were grown on pH 6 or pH 8 media for 5
978 days and then used for PM H⁺-ATPase H⁺-transport activity detection. D.
979 Acidification of transgenic apple calli. The 2-week-old transgenic calli were grown on
980 pH 6 or pH 8 media for 5 days and then transferred to bromocresol purple medium for
981 36 h. Acidification is indicated as a yellow color around the apple calli. E. Fe content
982 of WT, *MdbHLH104-OE/MdSIZ1-OE*, *MdbHLH104-OE*, *MdbHLH104^{K139R/K153R}-OE*,
983 and Control (*35S:GFP*) transgenic apple calli. The 2-week-old transgenic calli were

984 grown on pH 6 or pH 8 media for 5 days and then used for Fe content measurement.
985 DW, dry weight. F. Visualization of ferrous iron in WT, *MdbHLH104-OE/MdSIZ1-OE*,
986 *MdbHLH104-OE*, *MdbHLH104^{K139R/K153R}-OE*, and Control (*35S:GFP*) transgenic
987 apple calli. Ferrous iron is indicated by red-colored complex formed by the Ferrozine
988 reagent. G. Quantified measurements of ferrous complex of ferrozine in F. The optical
989 density (OD) of the complex was measured at 562 nm wavelength, and the
990 concentration of the complex was calculated according to Lambert-Beer law. Error
991 bars indicate the SD for three biological replicates in which the experiments were
992 carried out three times using the calli of each line. Samples denoted by different
993 letters are significantly different ($p < 0.01$, ANOVA, Tukey correction).

994 Figure 7. Transient silencing of *MdbHLH104* in the background of *MdSIZ1-OE*
995 partially inhibited its function in promoting PM H⁺-ATPase-mediated acidification
996 capacity and Fe homeostasis. A. Silencing of *MdbHLH104* by the *TRV-MdbHLH104*
997 vector in the background of *MdSIZ1-OE* transgenic calli. The *MdbHLH104* fragment
998 was amplified and cloned into the tobacco rattle virus (TRV) vector to transiently
999 silence the expression of *MdbHLH104* in the background of *MdSIZ1-OE* transgenic
1000 calli. The expression of *MdbHLH105* was used as a negative control. B. PM
1001 H⁺-ATPase H⁺-transport activity of WT, *MdSIZ1-OE*, *TRV-MdbHLH104/MdSIZ1-OE*,
1002 *TRV2/MdSIZ1-OE*, *antiMdSIZ1*, and Control (*35S:MYC*) transgenic apple calli. The
1003 2-week-old transgenic calli and the calli that had been treated with TRV were grown
1004 on pH 6 or pH 8 media for 5 days and then used for PM H⁺-ATPase H⁺-transport
1005 activity detection. C. Acidification of transgenic apple calli. The 2-week-old
1006 transgenic calli and the calli that had been treated by TRV were grown on pH 6 or pH
1007 8 media for 5 days and then transferred to bromocresol purple medium for 36 h.
1008 Acidification is indicated by the yellow color around the apple calli. D. Fe contents of
1009 WT, *MdSIZ1-OE*, *TRV-MdbHLH104/MdSIZ1-OE*, *TRV2/MdSIZ1-OE*, *antiMdSIZ1*,
1010 and Control (*35S:MYC*) transgenic apple calli. The 2-week-old transgenic calli and
1011 the calli that had been treated with TRV were grown on pH 6 or pH 8 media for 5
1012 days and then used for Fe content measurement. DW, dry weight. E. Visualization of
1013 ferrous iron in WT, *MdSIZ1-OE*, *TRV-MdbHLH104/MdSIZ1-OE*, *TRV2/MdSIZ1-OE*,
1014 *antiMdSIZ1*, and Control (*35S:MYC*) transgenic apple calli. Ferrous iron is indicated
1015 by the red-colored complex formed by Ferrozine reagent. F. Quantified measurements
1016 of ferrous complex of ferrozine in E. The OD of the complex was measured at 562 nm
1017 wavelength, and the concentration of the complex was calculated according to

1018 Lambert-Beer law. G. The expression of *MdAHA1*, *MdAHA3*, *MdAHA7*, *MdAHA8*,
1019 *MdAHA9*, *MdAHA11*, and *MdAHA12*, as measured by RT-qPCR, in WT and
1020 *MdSIZ1-OE* transgenic calli at pH 8. The two-week-old WT and *MdSIZ1-OE*
1021 transgenic calli were treated with pH 8 media and then used for gene expression
1022 detection. H. *MdAHA1*, *MdAHA8*, and *MdAHA9* expression in WT, *MdSIZ1-OE*,
1023 *TRV-MdbHLH104/MdSIZ1-OE*, *TRV2/MdSIZ1-OE*, and *antiMdSIZ1* transgenic apple
1024 calli under pH 8. The 2-week-old transgenic calli and the calli that had been treated by
1025 TRV were grown at pH 8 for 5 days and then used for gene expression detection. I.
1026 *MdFRO2* and *MdIRT1* expression in WT, *MdSIZ1-OE*,
1027 *TRV-MdbHLH104/MdSIZ1-OE*, *TRV2/MdSIZ1-OE*, and *antiMdSIZ1* apple calli at pH
1028 8. The 2-week-old transgenic calli and the calli that had been treated with TRV were
1029 treated with pH 8 media for 5 days and then used for gene expression detection. Error
1030 bars indicate the SD for three biological replicates in which the experiments were
1031 carried out three times using the calli of each line. Samples denoted by different
1032 letters are significantly different ($p < 0.01$, ANOVA, Tukey correction).

1033 Figure 8. A model of MdSIZ1-mediated sumoylation in the regulation the apple
1034 plant's response to Fe deficiency. Under Fe-deficient conditions, the sumoylation of
1035 MdbHLH104 and other unknown TFs mediated by MdSIZ1 promotes their protein
1036 stability. Stabilized TFs then bind to the promoters of PM H⁺-ATPases genes to
1037 promote the extrusion of protons to make Fe(III) more soluble. Meanwhile,
1038 MdbHLH104 also binds to the promoters of genes encoding Ib subgroup bHLH TFs,
1039 like *MdbHLH38* and *MdbHLH39*, to activate their expression. The sumoylation of
1040 MdbHLH104 mediated by MdSIZ1 thus promotes the expression of genes
1041 downstream of MdbHLH38 and MdbHLH39, such as *MdFRO2* and *MdIRT1*, which
1042 converts Fe³⁺ to Fe²⁺ and imports Fe²⁺ across the root epidermal cell membrane to
1043 improve tolerance towards Fe deficiency in apple plants. Under Fe-sufficient
1044 conditions, E3 ubiquitin ligase and MdbTs (i.e. MdbT1 and MdbT2) target
1045 MdbHLH104 and negatively regulate Fe absorption.

1046
1047

Parsed Citations

Baxter IR, Young JC, Armstrong G, Foster N, Bogenschutz N, Cordova T, Peer WA, Hazen SP, Murphy AS, Harper JF (2005) A plasma membrane H⁺-ATPase is required for the formation of proanthocyanidins in the seed coat endothelium of *Arabidopsis thaliana*. Proceedings of the National Academy of Sciences of the United States of America 102: 2649-2654

Pubmed: [Author and Title](#)

Google Scholar: [Author Only](#) [Title Only](#) [Author and Title](#)

Briat JF, Dubos C, Gaymard F (2015) Iron nutrition, biomass production, and plant product quality. Trends in Plant Science 20: 33-40

Pubmed: [Author and Title](#)

Google Scholar: [Author Only](#) [Title Only](#) [Author and Title](#)

Caesar K, Elgass K, Chen Z, Huppenberger P, Withhöft J, Schleifenbaum F, Blatt MR, Oecking C, Harter K (2011) A fast brassinolide-regulated response pathway in the plasma membrane of *Arabidopsis thaliana*. The Plant Journal 66: 528-540

Pubmed: [Author and Title](#)

Google Scholar: [Author Only](#) [Title Only](#) [Author and Title](#)

Catala R, Ouyang J, Abreu IA, Hu Y, Seo H, Zhang X, Chua NH (2007) The *Arabidopsis* E3 SUMO ligase SIZ1 regulates plant growth and drought responses. The Plant Cell 19: 2952-2966

Pubmed: [Author and Title](#)

Google Scholar: [Author Only](#) [Title Only](#) [Author and Title](#)

Colangelo EP, Guerinot ML (2004) The essential basic helix-loop-helix protein FIT1 is required for the iron deficiency response. The Plant Cell 16: 3400-3412

Pubmed: [Author and Title](#)

Google Scholar: [Author Only](#) [Title Only](#) [Author and Title](#)

Colby T, Matthäi A, Boeckelmann A, Stuible HP (2006) SUMO-conjugating and SUMO-deconjugating enzymes from *Arabidopsis*. Plant Physiology 142: 318-332

Pubmed: [Author and Title](#)

Google Scholar: [Author Only](#) [Title Only](#) [Author and Title](#)

Curie C, Briat JF (2003) Iron transport and signaling in plants. Annual Review of Plant Biology 54: 183-206

Pubmed: [Author and Title](#)

Google Scholar: [Author Only](#) [Title Only](#) [Author and Title](#)

Dalir N, Khoshgoftarmanesh AH, Massah A, Shariatmadari H (2017) Plasma membrane ATPase and H⁺ transport activities of microsomal membranes from wheat roots under Ni deficiency conditions as affected by exogenous histidine. Environmental and Experimental Botany 135: 56-62

Pubmed: [Author and Title](#)

Google Scholar: [Author Only](#) [Title Only](#) [Author and Title](#)

Flotho A, Melchior F (2013) Sumoylation: a regulatory protein modification in health and disease. Annual Review of Biochemistry 82: 357-385

Pubmed: [Author and Title](#)

Google Scholar: [Author Only](#) [Title Only](#) [Author and Title](#)

Fox TC, Guerinot ML (1998) Molecular biology of cation transport in plants. Annual Review of Plant Biology 49: 669-696

Pubmed: [Author and Title](#)

Google Scholar: [Author Only](#) [Title Only](#) [Author and Title](#)

Fuglsang AT, Guo Y, Cui TA, Qiu Q, Song C, Kristiansen KA, Bych K, Schulz A, Shabala S, Schumaker KS (2007) *Arabidopsis* protein kinase PKS5 inhibits the plasma membrane H⁺-ATPase by preventing interaction with 14-3-3 protein. The Plant Cell 19: 1617-1634

Pubmed: [Author and Title](#)

Google Scholar: [Author Only](#) [Title Only](#) [Author and Title](#)

Gill G (2004) SUMO and ubiquitin in the nucleus: different functions, similar mechanisms? Genes & Development 18: 2046-2059

Pubmed: [Author and Title](#)

Google Scholar: [Author Only](#) [Title Only](#) [Author and Title](#)

Guo CL, Chen Q, Zhao XL, Chen XQ, Zhao Y, Wang L, Li KZ, Yu YX, Chen LM (2013) Al-enhanced expression and interaction of 14-3-3 protein and plasma membrane H⁺-ATPase is related to Al-induced citrate secretion in an Al-resistant black soybean. Plant Molecular Biology Reporter 31: 1012-1024

Pubmed: [Author and Title](#)

Google Scholar: [Author Only](#) [Title Only](#) [Author and Title](#)

Gévaudant F, Duby G, von Stedingk E, Zhao R, Morsomme P, Boutry M (2007) Expression of a constitutively activated plasma membrane H⁺-ATPase alters plant development and increases salt tolerance. Plant Physiology 144: 1763-1776

Pubmed: [Author and Title](#)

Google Scholar: [Author Only](#) [Title Only](#) [Author and Title](#)

Hager A (2003) Role of the plasma membrane H⁺-ATPase in auxin-induced elongation growth: historical and new aspects. Journal of Plant Research 116: 483-505

Pubmed: [Author and Title](#)

Google Scholar: [Author Only](#) [Title Only](#) [Author and Title](#)

Hänsch R, Mendel RR (2009) Physiological functions of mineral micronutrients (Cu, Zn, Mn, Fe, Ni, Mo, B, Cl). Current Opinion in Plant Biology 12: 259-266

Pubmed: [Author and Title](#)

Google Scholar: [Author Only](#) [Title Only](#) [Author and Title](#)

Haruta M, Sussman MR (2012) The effect of a genetically reduced plasma membrane protonmotive force on vegetative growth of Arabidopsis. Plant Physiology 158: 1158-1171

Pubmed: [Author and Title](#)

Google Scholar: [Author Only](#) [Title Only](#) [Author and Title](#)

Hell R, Stephan UW (2003) Iron uptake, trafficking and homeostasis in plants. Planta 216: 541-551

Pubmed: [Author and Title](#)

Google Scholar: [Author Only](#) [Title Only](#) [Author and Title](#)

Hindt MN, Guerinet ML (2012) Getting a sense for signals: regulation of the plant iron deficiency response. Biochimica et Biophysica Acta (BBA)-Molecular Cell Research 1823: 1521-1530

Pubmed: [Author and Title](#)

Google Scholar: [Author Only](#) [Title Only](#) [Author and Title](#)

Hoagland DR, Arnon DI (1950) The water-culture method for growing plants without soil. Circular. California agricultural experiment station 347:1-38

Pubmed: [Author and Title](#)

Google Scholar: [Author Only](#) [Title Only](#) [Author and Title](#)

Huang L, Yang S, Zhang S, Liu M, Lai J, Qi Y, Shi S, Wang J, Wang Y, Xie Q (2009) The Arabidopsis SUMO E3 ligase AtMMS21, a homologue of NSE2/MMS21, regulates cell proliferation in the root. The Plant Journal 60: 666-678

Pubmed: [Author and Title](#)

Google Scholar: [Author Only](#) [Title Only](#) [Author and Title](#)

Ishida T, Yoshimura M, Miura K, Sugimoto K (2012) MMS21/HPY2 and SIZ1, two Arabidopsis SUMO E3 ligases, have distinct functions in development. PLoS One 7: e46897

Pubmed: [Author and Title](#)

Google Scholar: [Author Only](#) [Title Only](#) [Author and Title](#)

Janicka-Russak M, Kłobus G (2007) Modification of plasma membrane and vacuolar H⁺-ATPases in response to NaCl and ABA. Journal of Plant Physiology 164: 295-302

Pubmed: [Author and Title](#)

Google Scholar: [Author Only](#) [Title Only](#) [Author and Title](#)

Kim HS, Oh JM, Luan S, Carlson JE, Ahn SJ (2013) Cold stress causes rapid but differential changes in properties of plasma membrane H⁺-ATPase of camelina and rapeseed. Journal of Plant Physiology 170: 828-837

Pubmed: [Author and Title](#)

Google Scholar: [Author Only](#) [Title Only](#) [Author and Title](#)

Kobayashi T, Nishizawa NK (2012) Iron uptake, translocation, and regulation in higher plants. Annual Review of Plant Biology 63: 131-152

Pubmed: [Author and Title](#)

Google Scholar: [Author Only](#) [Title Only](#) [Author and Title](#)

Kobayashi T, Nagasaka S, Senoura T, Itai RN, Nakanishi H, Nishizawa NK (2013) Iron-binding haemerythrin RING ubiquitin ligases regulate plant iron responses and accumulation. Nature Communications 4: 2792

Pubmed: [Author and Title](#)

Google Scholar: [Author Only](#) [Title Only](#) [Author and Title](#)

Kobayashi T, Nakanishi H, Nishizawa NK (2010) Recent insights into iron homeostasis and their application in graminaceous crops. Proceedings of the Japan Academy, Series B 86: 900-913

Pubmed: [Author and Title](#)

Google Scholar: [Author Only](#) [Title Only](#) [Author and Title](#)

Leivar P, Monte E, Al-Sady B, Carle C, Storer A, Alonso JM, Ecker JR, Quail PH (2008) The Arabidopsis phytochrome-interacting factor PIF7, together with PIF3 and PIF4, regulates responses to prolonged red light by modulating phyB levels. The Plant Cell 20: 337-352

Pubmed: [Author and Title](#)

Google Scholar: [Author Only](#) [Title Only](#) [Author and Title](#)

Li X, Zhang H, Ai Q, Liang G, Yu D (2016) Two bHLH transcription factors, bHLH34 and bHLH104, regulate iron homeostasis in Arabidopsis thaliana. Plant Physiology 170: 2478-2493

Pubmed: [Author and Title](#)

Google Scholar: [Author Only](#) [Title Only](#) [Author and Title](#)

Lin XL, Niu D, Hu ZL, Kim DH, Jin YH, Cai B, Liu P, Miura K, Yun DJ, Kim WY (2016) An Arabidopsis SUMO E3 ligase, SIZ1, negatively regulates photomorphogenesis by promoting COP1 activity. PLoS Genetics 12: e1006016

Pubmed: [Author and Title](#)

Google Scholar: [Author Only](#) [Title Only](#) [Author and Title](#)

Ling HQ, Bauer P, Bereczky Z, Keller B, Ganai M (2002) The tomato fer gene encoding a bHLH protein controls iron-uptake responses in roots. *Proceedings of the National Academy of Sciences* 99: 13938-13943

Pubmed: [Author and Title](#)

Google Scholar: [Author Only](#) [Title Only](#) [Author and Title](#)

Li Z, Hu Q, Zhou M, Vandenbrink J, Li D, Menchyk N, Reighard S, Norris A, Liu H, Sun D (2013) Heterologous expression of OsSIZ1, a rice SUMO E3 ligase, enhances broad abiotic stress tolerance in transgenic creeping bentgrass. *Plant Biotechnology Journal* 11: 432-445

Pubmed: [Author and Title](#)

Google Scholar: [Author Only](#) [Title Only](#) [Author and Title](#)

Long TA, Tsukagoshi H, Busch W, Lahner B, Salt DE, Benfey PN (2010) The bHLH transcription factor POPEYE regulates response to iron deficiency in *Arabidopsis* roots. *The Plant Cell* 22: 2219-2236

Pubmed: [Author and Title](#)

Google Scholar: [Author Only](#) [Title Only](#) [Author and Title](#)

Mandadi KK, Misra A, Ren S, McKnight TD (2009) BT2, a BTB protein, mediates multiple responses to nutrients, stresses, and hormones in *Arabidopsis*. *Plant Physiology* 150: 1930-1939

Pubmed: [Author and Title](#)

Google Scholar: [Author Only](#) [Title Only](#) [Author and Title](#)

Miura K, Jin JB, Lee J, Yoo CY, Stirm V, Miura T, Ashworth EN, Bressan RA, Yun DJ, Hasegawa PM (2007) SIZ1-mediated sumoylation of ICE1 controls CBF3/DREB1A expression and freezing tolerance in *Arabidopsis*. *The Plant Cell* 19: 1403-1414

Pubmed: [Author and Title](#)

Google Scholar: [Author Only](#) [Title Only](#) [Author and Title](#)

Miura K, Lee J, Jin JB, Yoo CY, Miura T, Hasegawa PM (2009) Sumoylation of ABI5 by the *Arabidopsis* SUMO E3 ligase SIZ1 negatively regulates abscisic acid signaling. *Proceedings of the National Academy of Sciences* 106: 5418-5423

Pubmed: [Author and Title](#)

Google Scholar: [Author Only](#) [Title Only](#) [Author and Title](#)

Miura K, Rus A, Sharkhuu A, Yokoi S, Karthikeyan AS, Raghothama KG, Baek D, Koo YD, Jin JB, Bressan RA (2005) The *Arabidopsis* SUMO E3 ligase SIZ1 controls phosphate deficiency responses. *Proceedings of the National Academy of Sciences* 102: 7760-7765

Pubmed: [Author and Title](#)

Google Scholar: [Author Only](#) [Title Only](#) [Author and Title](#)

Mori S (1999) Iron acquisition by plants. *Current Opinion in Plant Biology* 2: 250-253

Pubmed: [Author and Title](#)

Google Scholar: [Author Only](#) [Title Only](#) [Author and Title](#)

Novatchkova M, Tomanov K, Hofmann K, Stuible HP, Bachmair A (2012) Update on sumoylation: defining core components of the plant SUMO conjugation system by phylogenetic comparison. *New Phytologist* 195: 23-31

Pubmed: [Author and Title](#)

Google Scholar: [Author Only](#) [Title Only](#) [Author and Title](#)

Park BS, Song JT, Seo HS (2011) *Arabidopsis* nitrate reductase activity is stimulated by the E3 SUMO ligase AtSIZ1. *Nature Communications* 2: 400

Pubmed: [Author and Title](#)

Google Scholar: [Author Only](#) [Title Only](#) [Author and Title](#)

Pinto SdS, Souza AEd, Oliva MA, Pereira EG (2016) Oxidative damage and photosynthetic impairment in tropical rice cultivars upon exposure to excess iron. *Scientia Agricola* 73: 217-226

Pubmed: [Author and Title](#)

Google Scholar: [Author Only](#) [Title Only](#) [Author and Title](#)

Robertson WR, Clark K, Young JC, Sussman MR (2004) An *Arabidopsis thaliana* plasma membrane proton pump is essential for pollen development. *Genetics* 168: 1677-1687

Pubmed: [Author and Title](#)

Google Scholar: [Author Only](#) [Title Only](#) [Author and Title](#)

Sampson DA, Wang M, Matunis MJ (2001) The small ubiquitin-like modifier-1 (SUMO-1) consensus sequence mediates Ubc9 binding and is essential for SUMO-1 modification. *Journal of Biological Chemistry* 276: 21664-21669

Pubmed: [Author and Title](#)

Google Scholar: [Author Only](#) [Title Only](#) [Author and Title](#)

Santi S, Schmidt W (2009) Dissecting iron deficiency-induced proton extrusion in *Arabidopsis* roots. *New Phytologist* 183: 1072-1084

Pubmed: [Author and Title](#)

Google Scholar: [Author Only](#) [Title Only](#) [Author and Title](#)

Steinacher R, Schär P (2005) Functionality of human thymine DNA glycosylase requires SUMO-regulated changes in protein conformation. *Current Biology* 15: 616-623

Pubmed: [Author and Title](#)

Google Scholar: [Author Only](#) [Title Only](#) [Author and Title](#)

Horsch RB (1985) A simple and general method for transferring genes into plants. *Science* 227: 1229

Pubmed: [Author and Title](#)

Google Scholar: [Author Only Title Only Author and Title](#)

Selote D, Samira R, Matthiadis A, Gillikin JW, Long TA (2015) Iron-binding E3 ligase mediates iron response in plants by targeting basic helix-loop-helix transcription factors. *Plant Physiology* 167: 273-286

Pubmed: [Author and Title](#)

Google Scholar: [Author Only Title Only Author and Title](#)

Shen H, He LF, Sasaki T, Yamamoto Y, Zheng SJ, Ligaba A, Yan XL, Ahn SJ, Yamaguchi M, Sasakawa H (2005) Citrate secretion coupled with the modulation of soybean root tip under aluminum stress. Up-regulation of transcription, translation, and threonine-oriented phosphorylation of plasma membrane H⁺-ATPase. *Plant Physiology* 138: 287-296

Pubmed: [Author and Title](#)

Google Scholar: [Author Only Title Only Author and Title](#)

Sibole JV, Cabot C, Michalke W, Poschenrieder C, Barceló J (2005) Relationship between expression of the PM H⁺-ATPase, growth and ion partitioning in the leaves of salt-treated *Medicago* species. *Planta* 221: 557-566

Pubmed: [Author and Title](#)

Google Scholar: [Author Only Title Only Author and Title](#)

Spartz AK, Ren H, Park MY, Grandt KN, Lee SH, Murphy AS, Sussman MR, Overvoorde PJ, Gray WM (2014) SAUR inhibition of PP2C-D phosphatases activates plasma membrane H⁺-ATPases to promote cell expansion in *Arabidopsis*. *The Plant Cell* 26: 2129-2142

Pubmed: [Author and Title](#)

Google Scholar: [Author Only Title Only Author and Title](#)

Stokey LL (1970) Ferrozine---a new spectrophotometric reagent for iron. *Analytical Chemistry* 42: 779-781

Pubmed: [Author and Title](#)

Google Scholar: [Author Only Title Only Author and Title](#)

Ulrich HD (2005) Mutual interactions between the SUMO and ubiquitin systems: a plea of no contest. *Trends in Cell Biology* 15: 525-532

Pubmed: [Author and Title](#)

Google Scholar: [Author Only Title Only Author and Title](#)

Walker EL, Connolly EL (2008) Time to pump iron: iron-deficiency-signaling mechanisms of higher plants. *Current opinion in plant biology* 11: 530-535

Pubmed: [Author and Title](#)

Google Scholar: [Author Only Title Only Author and Title](#)

Wang N, Cui Y, Liu Y, Fan H, Du J, Huang Z, Yuan Y, Wu H, Ling HQ (2013) Requirement and functional redundancy of Ib subgroup bHLH proteins for iron deficiency responses and uptake in *Arabidopsis thaliana*. *Molecular Plant* 6: 503-513

Pubmed: [Author and Title](#)

Google Scholar: [Author Only Title Only Author and Title](#)

Xie XB, Li S, Zhang RF, Zhao J, Chen YC, Zhao Q, Yao YX, You CX, Zhang XS, Hao YJ (2012) The bHLH transcription factor MdbHLH3 promotes anthocyanin accumulation and fruit colouration in response to low temperature in apples. *Plant, Cell & Environment* 35: 1884-1897

Pubmed: [Author and Title](#)

Google Scholar: [Author Only Title Only Author and Title](#)

Xu W, Jia L, Shi W, Baluška F, Kronzucker H, Liang J, Zhang J (2013) Tomato 14-3-3 protein TFT4 modulates proton efflux, basipetal auxin transport and PKS5-J3 pathway in root growth response to alkaline stress. *Plant Physiology*: pp. 113.224758

Pubmed: [Author and Title](#)

Google Scholar: [Author Only Title Only Author and Title](#)

Yang D, Chen D, Wang P, Jiang D, Xu H, Pang X, Chen L, Yu Y, Li K (2016) Aluminium-inhibited NO₃⁻ uptake is related to Al-increased H₂O₂ content and Al-decreased plasma membrane ATPase activity in the root tips of Al-sensitive black soybean. *Functional Plant Biology* 44: 198-207

Pubmed: [Author and Title](#)

Google Scholar: [Author Only Title Only Author and Title](#)

Yi Y, Guerinot ML (1996) Genetic evidence that induction of root Fe (III) chelate reductase activity is necessary for iron uptake under iron deficiency. *The Plant Journal* 10: 835-844

Pubmed: [Author and Title](#)

Google Scholar: [Author Only Title Only Author and Title](#)

Yi Y, Saleeba JA, Guerinot ML (1994) Iron uptake in *Arabidopsis thaliana*. *Biochemistry of Metal Micronutrients in the Rhizosphere*: 295-307

Pubmed: [Author and Title](#)

Google Scholar: [Author Only Title Only Author and Title](#)

Yu Y, Duan X, Ding X, Chen C, Zhu D, Yin K, Cao L, Song X, Zhu P, Li Q (2017) A novel AP2/ERF family transcription factor from *Glycine soja*, GsERF71, is a DNA binding protein that positively regulates alkaline stress tolerance in *Arabidopsis*. *Plant Molecular Biology* 94: 509-530

Pubmed: [Author and Title](#)

Google Scholar: [Author Only Title Only Author and Title](#)

Yuan KH (2005) Fit indices versus test statistics. *Multivariate Behavioral Research* 40: 115-148

Pubmed: [Author and Title](#)

Google Scholar: [Author Only](#) [Title Only](#) [Author and Title](#)

Yuan W, Zhang D, Song T, Xu F, Lin S, Xu W, Li Q, Zhu Y, Liang J, Zhang J (2017) Arabidopsis plasma membrane H⁺-ATPase genes *AHA2* and *AHA7* have distinct and overlapping roles in the modulation of root tip H⁺ efflux in response to low-phosphorus stress. *Journal of Experimental Botany* 68: 1731-1741

Pubmed: [Author and Title](#)

Google Scholar: [Author Only](#) [Title Only](#) [Author and Title](#)

Yuan Y, Wu H, Wang N, Li J, Zhao W, Du J, Wang D, Ling HQ (2008) FIT interacts with *AtbHLH38* and *AtbHLH39* in regulating iron uptake gene expression for iron homeostasis in Arabidopsis. *Cell Research* 18: 385

Pubmed: [Author and Title](#)

Google Scholar: [Author Only](#) [Title Only](#) [Author and Title](#)

Yavuz AS, Sezerman OU (2014) Predicting sumoylation sites using support vector machines based on various sequence features, conformational flexibility and disorder. *BMC Genomics* 15: S18

Pubmed: [Author and Title](#)

Google Scholar: [Author Only](#) [Title Only](#) [Author and Title](#)

Zhang J, Liu B, Li M, Feng D, Jin H, Wang P, Liu J, Xiong F, Wang J, Wang HB (2015) The bHLH transcription factor *bHLH104* interacts with *IAA-LEUCINE RESISTANT3* and modulates iron homeostasis in Arabidopsis. *The Plant Cell* 27: 787-805

Pubmed: [Author and Title](#)

Google Scholar: [Author Only](#) [Title Only](#) [Author and Title](#)

Zhao M, Song A, Li P, Chen S, Jiang J, Chen F (2014) A bHLH transcription factor regulates iron intake under Fe deficiency in *chrysanthemum*. *Scientific Reports* 4: 6694

Pubmed: [Author and Title](#)

Google Scholar: [Author Only](#) [Title Only](#) [Author and Title](#)

Zhao Q, Ren YR, Wang QJ, Yao YX, You CX, Hao YJ (2016) Overexpression of *MdbHLH104* gene enhances the tolerance to iron deficiency in apple. *Plant Biotechnology Journal* 14: 1633-1645

Pubmed: [Author and Title](#)

Google Scholar: [Author Only](#) [Title Only](#) [Author and Title](#)

Zhao Q, Ren YR, Wang QJ, Wang XF, You CX, Hao YJ (2016) Ubiquitination-related *MdBT* scaffold proteins target a bHLH transcription factor for iron homeostasis. *Plant Physiology* 172: 1973-1988

Pubmed: [Author and Title](#)

Google Scholar: [Author Only](#) [Title Only](#) [Author and Title](#)

Zheng Y, Schumaker KS, Guo Y (2012) Sumoylation of transcription factor *MYB30* by the small ubiquitin-like modifier E3 ligase *SIZ1* mediates abscisic acid response in Arabidopsis thaliana. *Proceedings of the National Academy of Sciences* 109: 12822-12827

Pubmed: [Author and Title](#)

Google Scholar: [Author Only](#) [Title Only](#) [Author and Title](#)

Zhou LJ, Li YY, Zhang RF, Zhang CL, Xie XB, Zhao C, Hao YJ (2017) The small ubiquitin-like modifier E3 ligase *MdSIZ1* promotes anthocyanin accumulation by sumoylating *MdMYB1* under low temperature conditions in apple. *Plant, Cell & Environment* 40: 2068-2080

Pubmed: [Author and Title](#)

Google Scholar: [Author Only](#) [Title Only](#) [Author and Title](#)